2015

MODELING AND ANALYZING THE DEFORMATION OF BALLAST STRUCTURES DUE TO REPETITION OF LOADS

A THESIS SUBMITTED TO SCHOOL OF CIVIL AND ENVIRONMENTAL ENGINEERING, ADDIS ABABA UNIVERSITY IN PARTIAL FULFILLMENT OF THE REQUIREMENTS FOR THE DEGREE OF MASTER OF SCIENCE IN CIVIL

ENGINEERING (RAILWAY ENGINEERING STREAM)

BY SHIMELIS ASSEFA

ADVISOR: MR. ABDULSATER SIRAJ (MSC)

DECEMBER 2015

2015

Addis Ababa University

Institute of Technology (AAIT)

School of Civil and Environmental Engineering

The undersigned hereby certify that they have read and recommend to Addis Ababa Institute of Technology for acceptance of a thesis titled **"Modeling and Analyzing the Deformation of ballast structure due to repetition of vehicles' loads"** by; Mr. Shimelis Assefa in partial fulfillment of the requirements for the degree of Masters of science.

Supervisor/Advisor:

1. _____ _____ _____

Signature Date

Examiner(s):

1. _____ _____ _____

Signature Date

2. _____ _____ _____

Signature Date

3. _____ _____ _____

Signature Date

DECLARATION

I, the undersigned, declared that this thesis is my own work and has not been presented in any other university. The work described in this thesis was conducted at the University of Addis Ababa, School of Civil and Environmental Engineering in partial fulfillment of the requirements for the degree of Master of Science in **Railway engineering**.

Declared by:

Name	Signature	Date
Shimelis Assefa	----------	29/12/2015

ACKNOWLEDGMENT

My greatest thank from the depth of my heart is to the Almighty God for endowing me with the courage, strength as well as health throughout the school time and for the successful accomplishment of this paper.

Next I would like to express my deepest gratitude and respect to my Advisor Abdulsater Siraj (MSc.) and Mr. Mequanent Mulugeta for their valuable contribution, assistance in providing relevant information, skills and encouragement for the accomplishment of this paper.

I also extend my thanks to all staff members of Civil and Environmental Engineering Departments, Railway Engineering Stream, of AAiT for their direct or indirect contributions on the successful completion of this paper.

ABSTRACT

The issue of permanent deformation of ballast structure due to repetition of loads is the most important element in railway maintenance planning and policy making. It affects the general operation and management of railway transportation plus the overall costs of track structure and its life spans.

To allow a safe, reliable and efficient rail network and to provide a good ride quality, the vertical profile of a railway track has to be maintained at a satisfactory level. And timely maintenance of ballast structure is essential to provide continuous service at reasonable costs since the track permanent deformation is a function of traffic load, environmental condition and track structure response behavior to the applied loads at different times of service life. Although most of the time deterioration process is very slow, but it might lead to massive failures with an enormous financial lose. This research determines the permanent deformation of railway ballast, particularly the vertical settlement under repeated traffic loading. Experimental data reviewed in the literature were assumed to represent the ballast materials used in LRT projects.

After initial elastic modeling, the extended Drucker-Prager model with hardening, which simulates the initial plastic deformation of granular materials under cyclic loads, were used in the FEM analysis in order to account for the inelastic behavior of railway ballast. Besides, FEM analysis provides the information to predict railway ballast deformation in terms of number of loading under wheel loading. And it can be observed that the vertical stresses were concentrated underneath the sleeper and ballast permanent deformation is increasing exponentially with increasing number of loading cycles and deform non- linearly with increasing depths of ballast.

Key Words:- Plastic deformation of ballast , Cyclic load, Numerical modeling

TABLE OF CONTENT

LIST OF TABLES

LIST OF FIGURES

LIST OF ABBREVIATION

C	constant
ε_N	permanent strain after a number of cycles (N)
N	number of cycle
ε_1	permanent strain after one cycle
n_p	Porosity
q	Deviator stress
p	confining stress
Mr	resilient modulus
$\varepsilon_{1,r}$	recoverable (resilient) axial strain during unloading
σ	Stress
E	Modulus of Elasticity
ε	Strain
LVDT	linear variable differential Transformer
ψ	dilation angle
DEM	discrete element method
FEM	Finite element method
$d\varepsilon^e_{ij}$	elastic strain increment
$d\varepsilon^p_{ij}$	plastic strain increment
β	the angle of the yield surface in p' – q stress space
σ_y (ε_{pl})	yield stress of materials
λ	plastic multiplier
ρ	Density of ballast
$\emptyset$	Friction angle of ballast
υ	Poisson's ratio
PEEQ	equivalent plastic strains
GUI	Graphical User Interface

CHAPTER ONE: INTRODUCTION

1.1 General Overview

Transportation is the back bone of once country in balancing the difference between the supply and demands for certain goods, information and passengers' flows. In combating the transportations problems different modes of transport are require at various corridor of the country. Due to its high capacity and high speed, rail transport, is more feasible for the country showing a population growing from time to times. Now a day's one of the transportation modes that the government of the Ethiopia starts to implement to reduce the transportation problems observed as a result of high population growth is railway mode of transports.

To allow a safe, reliable and efficient rail network and to provide a good ride quality, the vertical profile of a railway track has to be maintained at a satisfactory level. One area that has to be identified by railway corporations as financially expensive is the maintenance of the track substructure. In order to meet safety standards and to have acceptable ride quality the railway tracks require a specific level and alignment. Suiker et al. (2005) indicated that in conventional ballasted railway tracks, the level and alignment of the track structure strongly rely on the mechanical characteristics of the granular substructure, which is composed of a ballast layer, a subballast layer and subgrade layer. When track irregularities exceed allowable limits, either traffic speed restrictions or maintenance has to be carried out (Selig and Waters, 1994).

Although ballast usually comprises hard and strong angular particles, it undergoes gradual and continuing degradation under cyclic rail loading, which in turn increases settlement of the railway track. Particle degradation can also increase the magnitude of track settlement and accelerate

ballast fouling. The pumping of the subgrade clay is a major cause of ballast fouling. The fine particles either from clay pumping or ballast degradation increase the compressibility. The fine particles also fill the void spaces between larger aggregates and reduce the drainage characteristics of ballast. The fouling of ballast usually increases track settlement and may cause differential track settlement. In severe cases, fouled ballast needs to be cleaned or replaced to keep the track up to its desired stiffness, bearing capacity, alignment and level of safety. Prediction of differential permanent deformation under operational conditions is crucial to improve the railway system. However, the key limitation for prediction is our current poor understanding of ballasted track bed performance and the absence of a realistic stress-strain constitutive settlement model including plastic deformation under a large number of load cycles. The development of a proper scientific understanding of the dynamic load deformation response and granular ballast interactions would, therefore, have enormous benefits in the design of track systems, the development and maintenance strategies, the assessment of track system performance and the optimization of whole life and whole system costs.

It is important that railway structures provide adequate structural integrity to support the imposed loadings. The open granular track bed permits surface water entering along the rail and the joints within the surface to penetrate and subsequently saturate the underlying sub grade/roadbed, thus lowering the structural integrity of the structure support. Groundwater, if present due to inadequate drainage, can further lower the structural integrity of the track bed support layer. Permanent settlement occurs within the track structure imparting additional impact stresses and fatigue from railroad loadings. When the roughness and deterioration of the track adversely affects the safety and reasonable traffic operations across the track structures, the ballast structure must be removed and

replaced at high cost and inconvenience to the traveling public and railroad operations. Typically, the damaged ballast is replaced using similar materials and techniques, thus assuring a similar series of events. Therefore, timely maintenance of railway structure is essential to provide continuous service at reasonable costs. Increasing demand for higher traffic capacity (greater loads and traffic volume) shortens intervals between maintenance operations and increases costs. Track components become damaged due to dynamic excitation of rail traffics. Such excitation arises from the train vehicle running over track irregularities. Provided that a sufficient number of trains' vehicles pass over a site at a similar speed, the dynamic contact loads between rail, sleeper and ballast are similar from one train to another. The same irregularities excite each train and the damages caused by rolling vehicles tend to exacerbate vibration of subsequent vehicles leading to further damages.

Generally, to enhance the service life of track structure after commissioning, it needs to know the permanent deformation of ballast structures due to repetitions of vehicle loads. The interactive forces between moving vehicle and track (via wheel/rail contacts) and track responses depend on the dynamic properties (parameters) of the two, and also on the vehicle speed, track components and wheel defects. Therefore, it is very important to understand the behavior of track (specifically behavior of ballast in this paper), and to find important parameters, which reduces the dynamic responses of track components.

1.2. Statement of problem

When a ballasted rail track structures are subjected to repeated vehicle loads, called cyclic loads, the resulting cyclic stresses can lead to microscopic physical damage to the materials involved. Although ballast is usually comprised of hard and strong angular particles, which are derived from high strength unweathered rocks, it also undergoes gradual and continuing degradation under cyclic loading. Even at stresses below the material's ultimate strength, this damage can accumulate with continued cycling until it develops into a settlement or other damage that leads to failure of the components. The sharp age and corners are broken due to high stress concentrations at the contact points between adjacent particles. The reduction in angularity decrease its angle of internal friction (i.e. shear strength), which in turn increases plastic settlement of the track.

Although most of the time deterioration process is very slow, but it might lead to massive failures with an enormous financial lose. As a result it is very important to decide what causes track deterioration, when and how to perform maintenance operations for the systems and how to allocate the resources (manpower, materials, machines and funds) to the parts of the system with highest need. Based on the demand for transportation Ethiopian Railway Corporation has carried out the national and light rail transit (LRT) project construction. But both LRT and national projects are implementing the ballasted track, which is more sensitive to repetition of traffic loads, rather than slab track. Under repeated vehicles loading, ballast layer exhibits both recoverable and unrecoverable deformation. When the unrecoverable ballast deformation increases to cause considerable settlement and stability problems, maintenance activities such as tamping are performed to maintain the track level.

1.3. Research Objectives

The need to understand the deterioration behavior of railway ballast and to be able to model its behavior is increasingly important in order to ensure the safety of the train operation and to enhance the durability of the track structures. This research will employ the modeling and analyzing the effect of vehicle repetitions on the ballast layer.

1.3.1. General Objectives:

The general purpose of this study is that to model and analyses the effect of vehicle repetitions on the ballast layer and in order to quantify the permanent deformation of ballast layer due to, N, number of vehicle repetition loads.

1.3.2. The specific objectives are to:

- Simulate the ballast sample used in trail axial test with the Abacus software.
- Quantify the permanent deformation (settlement) of ballast materials subjected to cyclic vehicle loading and analyze the stress and strain distribution in ballast structure.
- To compare the experimental and numerical permanent deformation results of ballast materials after, N, number of vehicle repetition.

1.4. Significance of the Research

This thesis enhances the awareness of railway track designer in optimising the depth of ballast layer to withstand the effect of repetition of loads. In additions, it offers the special maintenance consideration for ballast settlement due to repetition of vehicles to enhance the durability of tracks or it will benefit the design of appropriate maintenance and renewal strategies.

1.5. Scope of the Thesis

From railway track structure under consideration in this paper, only ballast deformation is modelled and analysed since it is more sensitive to vehicle repetitions loads. Also in this paper only numerical modelling is performed due to limitation of test machines and financial constraint. More emphasis is given for the modelling and analyzing the permanent deformation of ballast layer under the cyclic loading and comparing numerically determined permanent deformation of ballast after, N, number of load repetitions with permanent deformation of ballast determined using empirical modelling. Only numerical modelling is performed by taking the required input data from the literatures due to lack of trail axial machine to conduct the laboratory tests.

1.6. Organization of the Thesis

This thesis is divided into five chapters. A summary of the remaining chapters is given below. Following this introductory chapter 1, Chapter 2, a literature review, begins with introduction to degradation mechanism of track structures especially the general Overviews of resilient and permanent deformations of ballast materials are presented in the same section. An introduction to the various types of railway settlement mathematical models and various factors affecting the deformation of ballast materials is presented in the next section. Lastly, the behavior of ballast materials under cyclic loading and its simulation under the trail axial test were reviewed.

In Chapter 3, the introduction of ballast deformation and modeling technique of ballast materials are introduced. Especially, elasto plastic behavior of ballast and Extended Drucker-Prager Modeling technique is presented.

Chapter 4 presents, the modeling procedures and simulation of ballast materials in the finite element softwares, ABAQUS. And finally the main findings and discussion of this research study, and empirical settlement prediction after, N, number of load cycles are interpreted in chapter five.

Chapter 6 describes the general conclusion of the research findings and recommendations for further research (study). And it is the chapter that is followed by a list of references.

CHAPTER 2:- REVIEW OF RELATED LITERATURE

2.1. Introduction to railway track degradation mechanisms

Deterioration of the vertical and lateral geometry of the track takes place due to settlement and disturbance of the ballast and sub grade, predominantly as a result of traffic. Uniform settlement or uniform shift in the lateral case would not itself cause deterioration, but it is the differential movements which result in a worsening of passenger ride and an increase in dynamic loads. Differential displacements can occur due to the general random nature of the settlement process and also due to the lack of straightness of the rails, but the major contributor to the problem is the vehicle cyclic loads. The magnitude of settlement in the ballast depends upon magnitude of axle load, number of loading cycles, speed & percentage content of fouling material (i.e. undesirable fine material of size 9.5 mm or less)

2.1.1. Ballast Deterioration

Ballast Fouling:- Ballast fouling, which is a major degradation mode, is a process of ballast voids being filled with fines, from either ballast particle abrasion or foreign substance intrusion such as windblown dust, spillage from wagons, and pumped fine from underlying subgrade. Most research suggests that the majority of fines are from the ballast itself, as a result of abrasion, impact and physical and chemical weathering (e.g.. Selig, Collingwood and Field, 1988). The fouling process is influenced by track loading, particle size distribution, particle shape and particle surface characteristics.

Ballast fouling is not considered to be significant until the amount of fines (particles of diameter smaller than 0.075mm) reaches 10 percent or more (Selig, 1985). When ballast voids

are completely filled with fines, the ballast becomes deformable when wet, and stiff when dry (or frozen in cool weather), preventing proper track surfacing.

In order to reduce ballast fouling, in practice, ballast cleaning and replacement with fresh ballast should be carried out. If the ballast is extremely dirty, it may need to be totally replaced. The contamination problem requires the use of ballast with high crushing resistance.

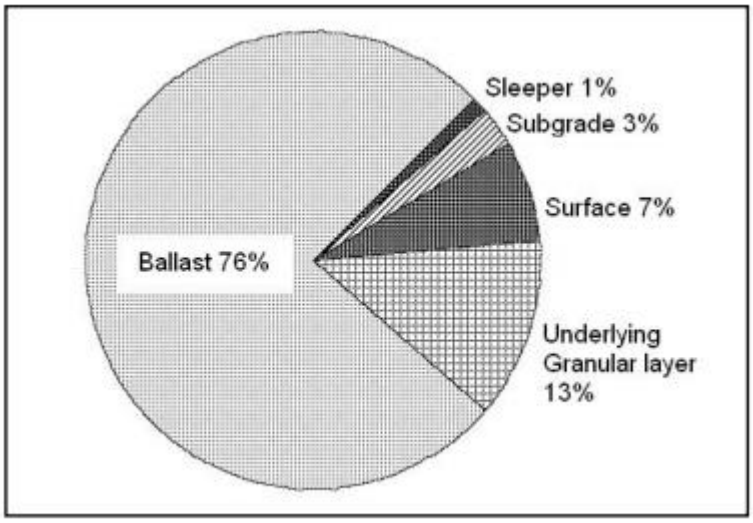

Figure- 2.2. Major source of ballast fouling (Selig and Waters, 1994)

When the track geometry deterioration due to settlement of ballast becomes unacceptable, tamping is employed to re-establish the desired track geometry. However, tamping process loosens the ballast and causes ballast breakage. Therefore, more settlement occurs as ballast is re-compacted under train loading. This causes faster deterioration of track geometry and leading to increase in frequency of tamping & maintenance effort.

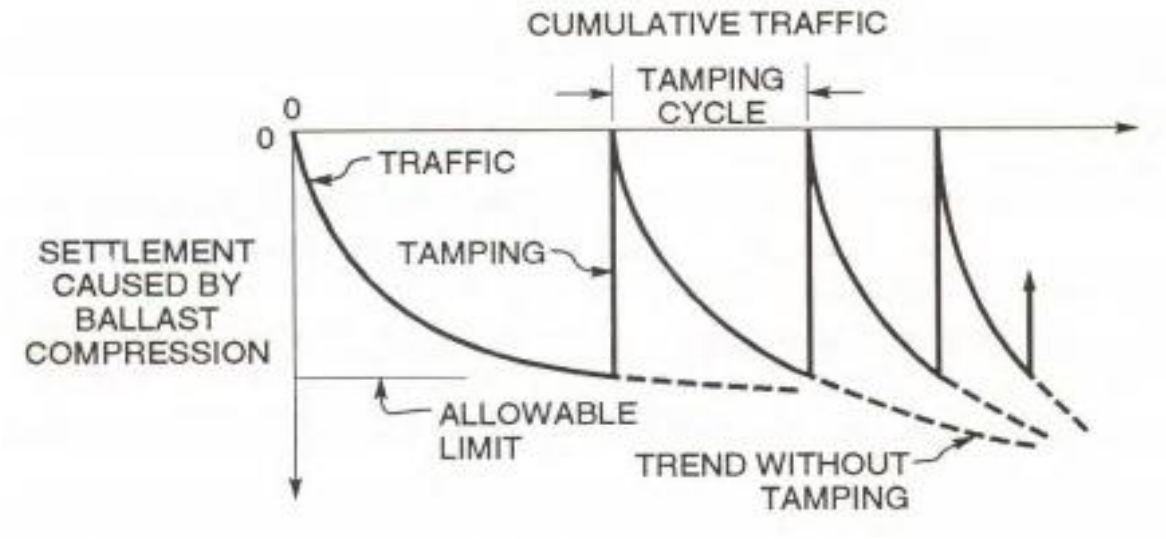

Figure 2.3. Deformation in tamping cycle with increase in fouling of ballast (Source: Selig and Waters 1994)

2.1.2. Ballast Specifications

Ideally, ballast used for railway track should have high stiffness, high strength, crushing resistance, chemical resistance and be free from dust. High stiffness can reduce stress to weaker underlying materials, reduce track deflection under load and reduce bending stresses in the rails. The reason for high strength is to reduce build-up of deformation under traffic loading and impart horizontal stability to the track. Besides these functions, ideal ballast should not be affected by dirt from above, soil contamination from below, rainfall, frost and chemical weathering.

Additionally, ballast should absorb noise and surplus energy from vibration, meanwhile, allow easy maintenance and be sufficiently workable. The strength of ballast particles is probably the most important factor directly governing ballast degradation, and indirectly settlement and lateral deformation of the railway track (Salim, 2004). If an individual particle is

overstressed, it will fracture and the ballast particles will re-orientate themselves. Fracturing will continue until re-orientation is completed, meaning that there is enough particle contacts for each not to be at too high a stress.

The mechanical behavior of ballast is affected by the particle size. Indraratna et al. (1998) indicated that the peak friction angle decreased slightly with an increasing grain size at confining pressures which were less than 300kPa. The effect of particle size on friction angle became negligible when the stress was over 400kPa. Raymond and Diyaljee (1979) concluded that smaller ballast particles deformed less when the stress level did not exceed a critical value. However, smaller ballast particle size had lower final compaction strength than larger ballast. Selig (1984) recommended that the ideal ballast should be of 10-50mm size with some particles beyond this range. The larger particles stabilize the track and the smaller particles reduce the contact forces between particles and minimize breakage. Ballast dimensions recommended to be used from the 1st April 2005 are shown in Figure 2.8. From this figure, it can be seen that the track ballast should have a consistent mixture of sizes mainly between 32mm and 50mm.

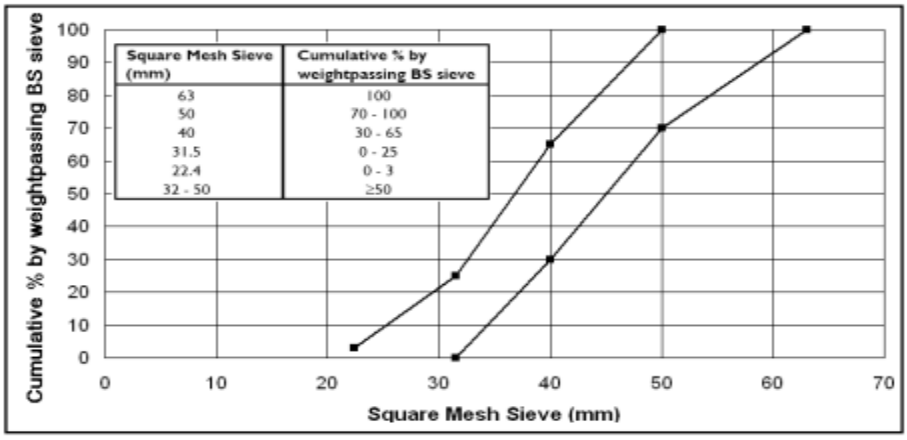

Figure 2.4 Specification for ballast particle size distribution (RT/CE/S/006, 2000)

2.1.3. Ballast Deformation Mechanisms

Railway track will settle as a result of permanent deformation in the ballast and underlying soil caused by repeated traffic loading. Permanent deformation of track structure results from several mechanisms of ballast and sub grade behavior.

Some mechanisms are:

- Volume reduction or densification caused by particle rearrangement.
- Inelastic recovery on unloading or stress removal.
- Volume reduction caused by particle breakdown from loading or environmental factors.
- Sub grade penetration into ballast voids. This causes the ballast to sink into the sub grade.

The vertical downward forces at the rail-wheel contact points tend to lift up the rail and sleeper some distance away from the contact point (Selig and Waters, 1994). As the wheel advances, the lifted sleeper is forced downward causing an impact load, which increases with increasing train speed. This movement causes a pumping action in the ballast, which increases the ballast settlement by exerting a higher force on the ballast and causing “pumping up” of fouling materials from the underlying materials in the presence of water. The increase of impact load leads to an increase in ballast settlement and to a larger gap underneath the sleeper. According to Selig and Waters (1994) ballast breakage constitutes 76% of the source of ballast fouling material, while the minor sources of fouling materials are infiltration from underlying granular layer and surface, sub grade infiltration or sleeper wear (Fig. 2.1). Festag and Katzenbach (2001) defined particle breakage as the dissection of grains into parts with nearly

the same dimension and the probability of particle breakage in an aggregate increase with an increase in applied macroscopic stress and particle size, and reduction in coordination number (i.e., number of contacts with neighboring particles).

Also Selig and Waters (1994) concluded that there were two main modes in which granular material deformed: frictional slip and particle breakdown. During each passing axle load, either of these modes of deformation can be occurring at a different point within the ballast. They are interdependent mechanisms causing the ballast to be a continually changing material. The key form of deformation is frictional slip between ballast particles. It should be noted that frictional slip does not only imply permanent deformation, but it takes place during normal repeated loading as well, first one way then back again. However, a small part of the slip is not recovered each time, which forms the permanent deformation. Ballast particles slip back to release the energy stored elsewhere. Liao et al. (1995) defined slip as the relative motion of particles in contact under applied load.

Ballast abrasion is a phenomenon where very small particles break off from the grain surface. Festag and Katzenbach (2001) indicated that ballast abrasion took place when the particles slipped or rolled over each other during shear deformation, and might occur even at low stress level. . Also they defined that, particle breakage as the dissection of grains into parts with nearly the same dimension and stated that it generally occurred in the high stress domain.

Thom (2005) concluded that the vehicle load caused a certain percentage of ballast particle breakage in addition to ballast contact slip. Grain breakage might be absent if the stress level was low compared to particle strength.

Various researchers have empirically modeled the permanent deformation of ballast under cyclic loading. Alva-Hurtado and Selig (1981) related the permanent strain (ε_N) after a number of cycles (N) to the permanent strain after one cycle (ε_1) through the following expression:

$$\varepsilon_N = \varepsilon_1 (1+ClogN) \quad \text{.....Equation (2.1)}$$

Where, C is a dimensionless constant controlling the rate of the deformation growth between 0.2 and 0.4 (Selig and Waterd, 1994). ε_1 is the permanent strain caused by the first load cycle and it was proposed by:

$$\varepsilon_1 = 0.082(100n_p - 38.2)(\sigma_1 - \sigma_3)^2 \quad \text{---------- Equation (2.2)}$$

Equation (2.2) can be used to relate the permanent axial strain to the ballast condition (Porosity) and the number and magnitude of the applied axial load cycles. Typical values for porosity are between 0.4 and 0.5. For slag the porosity value is 0.34, for granite it is 0.26 and for limestone it is 0.4 (Steward and Selig, 1982)

SHI (2009) conducts several triaxial tests on different ballast samples, each submitted to 100000 cycles of axial loading-unloading with a growing-in-time frequency of load application. And he obtained diagrams of permanent deformations versus the number of cycle N, revealed that when N is less than 10000 permanent deformations are important, and for N above 1000000, the accumulation of permanent deformations is very slow and a linear relationship between these variables is observed. Furthermore, ballast particle breakage is linearly related to permanent axial strain in cyclic triaxial tests after 100,000 cycles and before failure.

The influence of stress level on permanent accumulated strain after a certain number of repeated loads is directly related to the ratio of deviator stress q to confining stress p.

Increasing the stress ratio q/p increases the permanent strain and, for the same stress ratio, increasing the stress path-length increases the ratio $(q/p)_{max}$ and the amount of permanent strain accumulated (Lekarp et al., 2000; SHI, 2009) up to sample failure.

Also Xiaoyi Shi (april2009) Conducted two trail axial tests under confining pressure of, 10kPa, 30kPa and 60kPa, a total of six tests, and he obtained that, with the same cell pressure, permanent axial strain increases with increasing maximum stress ratio ((q/p)max) .With the same (q/p)max, the sample deforms more at increased cell pressure.

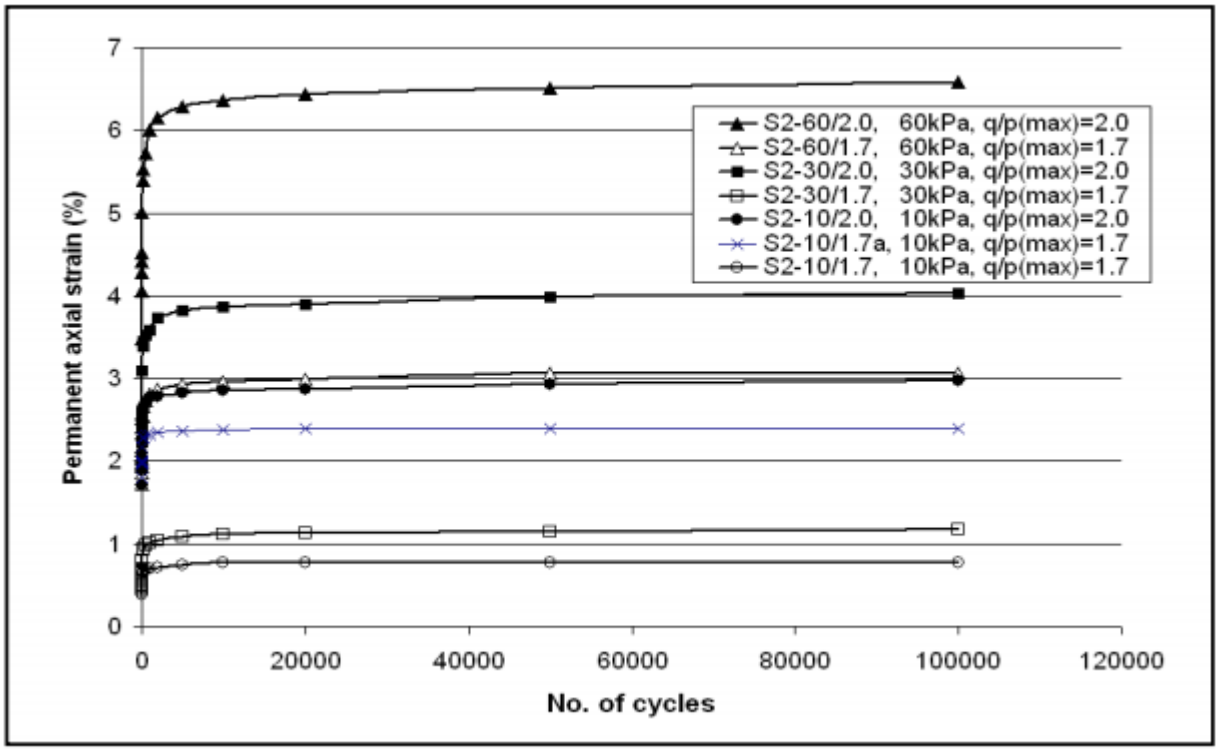

Figure 2.5. Permanent axial strain versus number of cycles (source: Xiaoyi Shi, 2009)

2.2. Resilient Behavior of Ballast Material under cyclic loading

In a granular material such as ballast, plastic deformations occur under repeated traffic loads. The vertical component of the plastic deformation results in track settlement. Because the material within the layer is confined, the stresses in the unloaded state will also progressively change under the effects of the repeated load. Progressive volume change under repeated wheel loading causing vertical deformation occurs because of particle rearrangement to a more dense packing state and particle breakage, with the smaller particles moving into the voids of the larger particles. Therefore, track settlement is the result of the compression of the substructure layers under repeated wheel loads.

When ballast structures are subjected to repeated vehicle loads, called cyclic loads, the resulting cyclic stresses can lead to microscopic physical damage to the materials involved. Even at stresses below the material's ultimate strength, this damage can accumulate with continued cycling until it develops into a break or other damage that leads to failure of the component. And this process of accumulating damage and finally to failure due to cyclic loading is called fatigue. Figure 2.6 shows the stress-strain behavior of the ballast. The resilient modulus represents the ultimate stiffness of the materials, and the accumulated plastic strain under repeated loading.

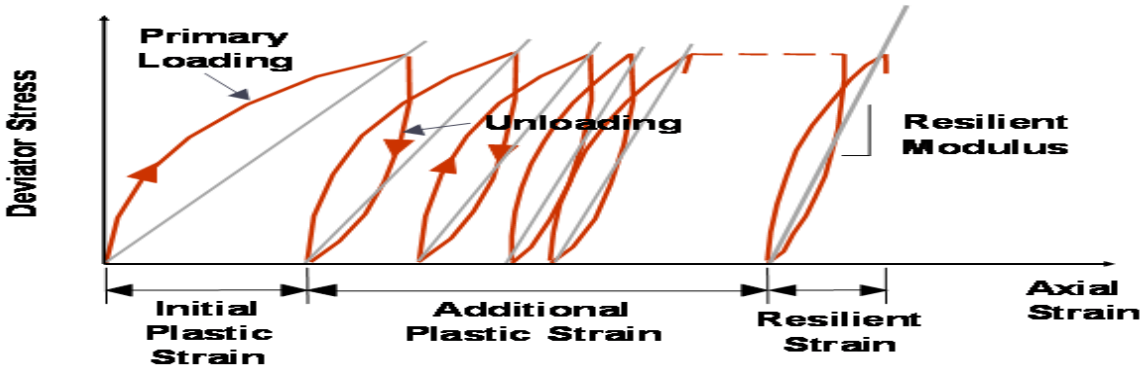

Figure 2.6: The stress-strain behavior of the ballast under cyclic loading

The deformation response of ballast material under repeated loading is commonly characterized by a permanent deformation as well as a recoverable resilient deformation. During each traffic cycle, the difference between the maximum strain exerted from the peak load and the permanent strain when the ballast is unloaded is recoverable strain, which is known as the resilient strain, as illustrated in Figure 2.7. The resilient modulus can be calculated as the repeated deviator stress divided by the recoverable axial strain during unloading in the tri axial test (Seed et al., 1962) as shown in the equation below:

$$Mr = \frac{q}{\varepsilon 1,r} \text{ ---------- (Equation 2.2)}$$

Where Mr = resilient modulus,

q = transient deviator stress = σ_1'-σ_3'

$\varepsilon_{1,r}$ = recoverable (resilient) axial strain during unloading.

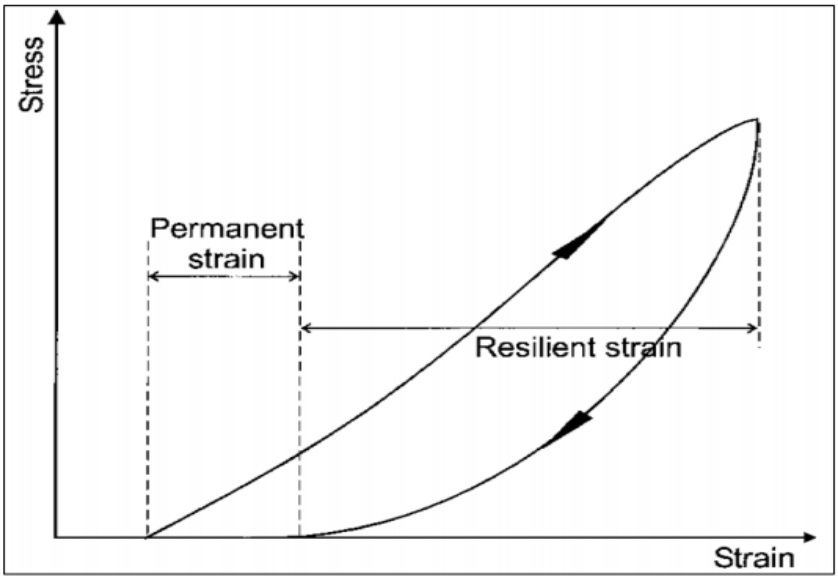

Figure 2.7. Strains in granular materials during one cycle of load application (Wright, 1983)

The resilient behavior of granular material may be affected by several factors such as: stress state, stress history, loading sequence, number of loading cycles, aggregate type, geometry (shape and texture), aggregate grading and moisture content.

The major effect on resilient behavior is stress, including stress state, stress history and stress sequence. Lekarp et al., (2000a) agreed that the resilient modulus increased considerably with an increase in confining pressure and sum of principal stresses, which has been agreed by many researchers (e.g. Hicks and Monismith, 1971; Uzan, 1985; Thom and Brown, 1989; Sweere, 1990). Hicks and Monismith (1971) concluded that the predominant factor affecting resilient modulus was the bulk stress (the sum of the three principal stresses with the maximum load applied), and the resilient modulus was expressed as a function of the sum of principal stresses or bulk stress in the loaded state.

From triaxial tests on well graded crushed basalt, Rowshanzamir (1995) concluded that the loading sequence did not affect resiliency. Similar results have been reported by Raad and

Figueroa (1980). Dehlen (1969) reported that resilient modulus could be affected by stress history as a consequence of progressive densification, particle rearrangement, and the development and dissipation of excess pore water pressure.

The amount of resilient strain generally decreases with number of cycles, i.e. the resilient modulus increases gradually with the number of repeated load applications. Eventually, the resilient modulus comes to an approximately constant value after a certain number of repeated loads and the material behaves in an almost purely resilient manner. Selig and Waters (1994) studied the change of the resilient modulus over a number of load applications in a triaxial apparatus, as shown in Figure 2.8. It appears that the amount of resilient strain generally decreases with number of cycles, which is similar to the findings of other researchers (e.g. Dehlen, 1969; Brown, 1974; Khedr, 1985).

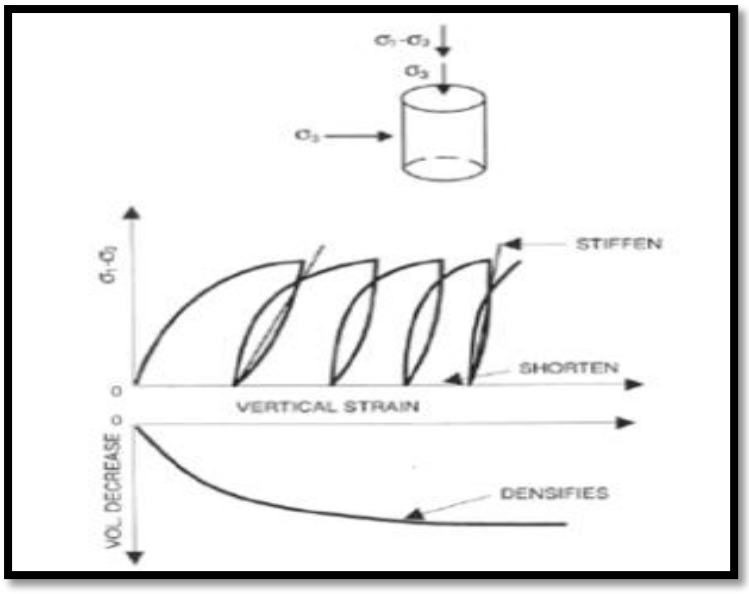

Figure 2.8. Ballast behavior in the cyclic triaxial test (Selig and Waters, 1994)

Referring to aggregate type, Zaman et al. (1994) subjected six materials (three lime stones, sandstone, granite and rhyolite) to cyclic loading and found that the type of aggregate

significantly influenced the resilient response, with the resilient modulus for the various materials differing by 20-50%. Many researchers (e.g. Allen and Thompson, 1974; Yoder and Witczak, 1975; Barksdale and Itani, 1989) found that the resilient modulus was enhanced when the particle shape became more angular and the texture rougher. Thom and Brown (1989) have reported that crushed aggregate, having angular to sub angular shaped particles, provides better load spreading properties and a higher resilient modulus than uncrushed gravel with sub rounded and rounded particles.

The effect of grading on the resilient modulus has been deemed minor when compared to other influences. Zaman et al. (1994) witnessed an insignificant change (< 10%) in resilient modulus when the coefficient of uniformity (Cu) was increased from 43.3 to 65.6. Thom and Brown (1988) studied the effect of grading on the shear stiffness of crushed limestone and identified that uniform specimens were marginally stiffer. Knutson and Thompson (1977) indicated that well graded ballast had a slightly higher resilient modulus than the more uniform ballast.

Besides the influences above, Lekarp et al., (2000a) also reported that the effect of moisture on resilient modulus depended on the degree of saturation. At low degrees of saturation, the moisture content has negligible effect on resilient modulus. However, the resilient modulus decreases considerably for high degrees of saturation, especially as the aggregate approaches complete saturation.

2.3. Elastic Behavior of ballast materials

Fully elastic deformation is defined as reversible alteration of the form or dimensions of a solid body under stress or strain. In the elastic range, the part will be stressed but will maintain its ability to return to its original shape. The stability of the bonds will ensure the material will not

plastically deform but once the internal energy is enough to break the bonds there will be permanent deformation.

Fully elastic deformation is typically governed by Hookes Law that states:

$\sigma = \varepsilon E$ Where: σ= Stress

E = Modulus of Elasticity

ε= Strain

Hooke's law is a linear relationship that relates stress to strain by using the modulus of elasticity of the material. Fully elastic analysis only pertains to stress and strain up to the yield point.

In FEA, to analyze items within the fully elastic range only the modulus of elasticity and material density are required to perform a structural analysis. The analysis is assumed to be accurate up to yield point but will continue to act linearly beyond the yield point. The linear relationship past the yield point will result in an inaccurate result for high stresses and high strains.

2.4. Ballast sample Simulation

2.4.1. Initial Box Test Simulation

Box tests were handled by Lim (2004) at the University of Nottingham to represent a volume of ballast below a section of sleeper underneath the rail seat. He considers the box having a length of 700mm, width of 300mm and height of 450mm. The base of the box consists of a 10mm thick rubber sheet to replicate typical foundation stiffness. To set up a test, a 300mm thick layer of ballast is first placed in the box, tamped and leveled. He placed a 300mm long, 250mm wide and 150mm high rectangular hollow steel section on top of the ballast and surrounded by further

overburden ballast. A schematic diagram and a photograph of the box test rig are shown in Figures 2.9 (a) and (b).

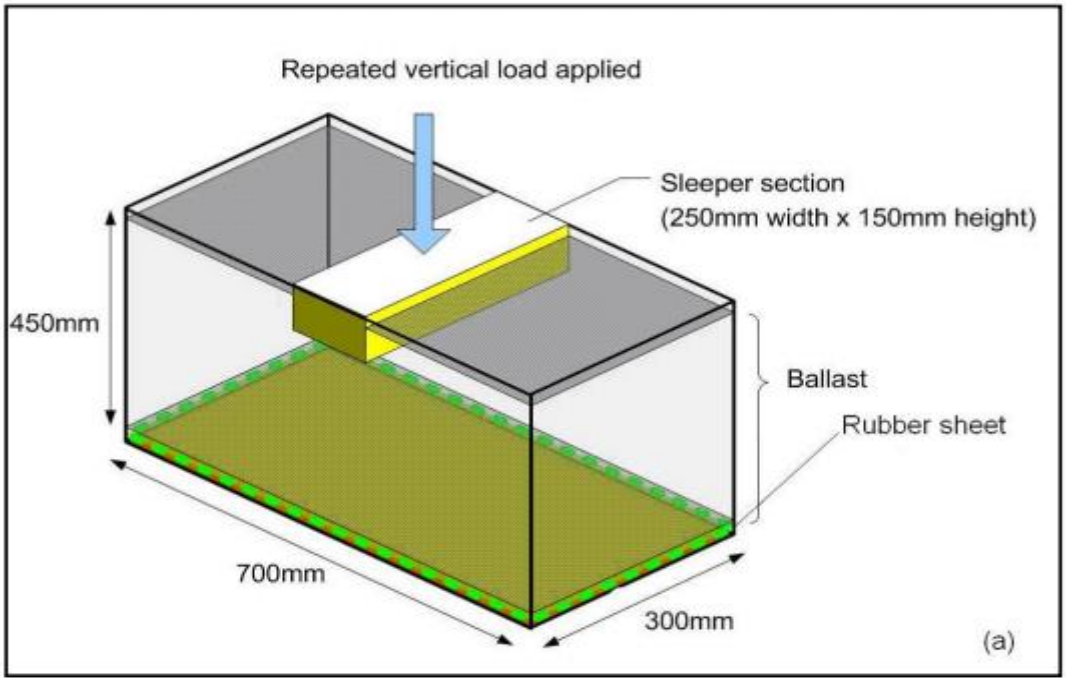

Figure 2.9. (a) Schematic diagram of the Initial box test (Source: Xiaoyi Shi)

Figure 2.9 (b) the initial box test set-ups (Source: Xiaoyi Shi)

He used a linear variable differential Transformer (LVDT) mounted on the sleeper to measure the ballast settlement. The load cell attached to the actuator records the load values. Instrument arrangement details can be found in Figure 2.9 (b). Lim (2004) carried out the test with a minimum load of 3kN and a maximum load of 40kN for 1,000,000 cycles with a frequency of 3Hz. In addition, Li et al. (2007) carried out box tests on various interlayer systems with a 25kN peak load for up to 1,000,000 cycles with a frequency of 5.5Hz.

2.5. Elasto plastic Material Model

Plastic deformation is defined as permanent change in shape or size of a solid body without fracture resulting from the application of sustained stress beyond the elastic limit. Plasticity will occur beyond the yield point of the material. Once the load exceeds the yield strength threshold, there is more of a rapid increase in stress than in the elastic range, and when the load is removed some amount of the extensions will exist which results in permanent deformation.

Elasto-plastic analysis uses the Modulus of Elasticity from the elastic material properties but FEA ABAQUS requires yield stress and plastic strains of the material in the plastic range to be manually loaded into the material properties. If the plasticity data has not been entered into FEA ABAQUS, the stress/strain relationship will continue to be linear. This will not provide an accurate result of stress in the plastic range. More experimental data needs to be obtained to validate the numerical solutions. FEA is a method of using the experimental data from plastic deformation (yield stress and plastic strain) and analyzing the deformation in the plastic range. As a result, this reduces the number of assumptions and leads to a more accurate result.

The monotonic triaxial test results were used to validate the parameters in elasto plastic material modelling. Since there were three extended Drucker-Prager yield criteria are provided in Abaqus : a linear form, a hyperbolic form and a general exponent form, the linear model were primarily used by Xiaoyi Shi (April2009) for applications where the stresses are for the most part compressive. The yield function with linear form is given by:

$$Fs = q + \alpha p' - \sigma_y(\varepsilon_{pl}) = 0 \quad \ldots\ldots\ldots\ldots (2.1)$$

The parameter α can be obtained by matching experimental triaxial test data. And the initial yield points from the monotonic triaxial tests in figure 2.10 could be plotted in the meridional plane as shown in figure 2.11

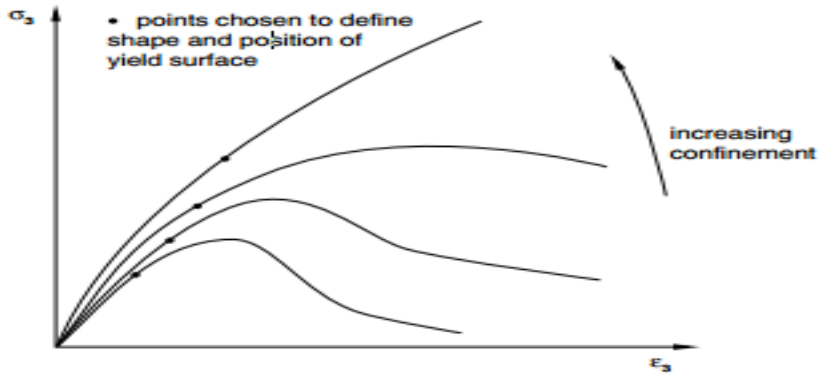

Figure 2.10. Points chosen to define the shape and position of the initial yield surface

(Source: Abaqus software manual)

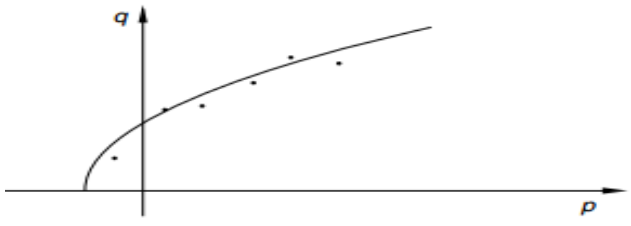

Figure 2.11. Initial yield surface plotted in the Meridional plane

(Source: Abaqus software manual)

In order to have better representation, Xiaoyi Shi defined the virtual Uniaxial stress-strain curves of the ballast independently at different cell pressures to account the Multi-linear Isotropic Harding (MISO) of ballast as shown in table 2.1 below.

Table 2.1. Virtual uniaxial stress-strain curve for hardening simulation

For Cell Pressure =5kPa		For Cell Pressure =10kPa	
Strain	Pressure (pa)	Strain	Pressure (pa)
0.0005	4850	0.0005	7700
0.008	15000	0.008	20000
0.02	20000	0.02	25000
0.04	26000	0.04	36000
0.06	29500	0.06	39000
0.09	30500	0.09	42000
0.15	31500	0.15	44000
For Cell Pressure =30kPa		For Cell Pressure =60kPa	
Strain	Pressure (pa)	Strain	Pressure (pa)
0.005	30000	0.005	33000
0.008	46000	0.008	61000
0.02	55000	0.02	92000
0.04	77000	0.04	108000

0.06	85000	0.06	130000
0.09	91000	0.09	161000
0.15	92000	0.15	174000

The MISO option uses the von Mises yield criteria coupled with an isotropic work hardening assumption. This option is often preferred for large strain analyses, and it is defined by the uniaxial stress-strain test results in Abaqus, as shown in Figure 2.12.

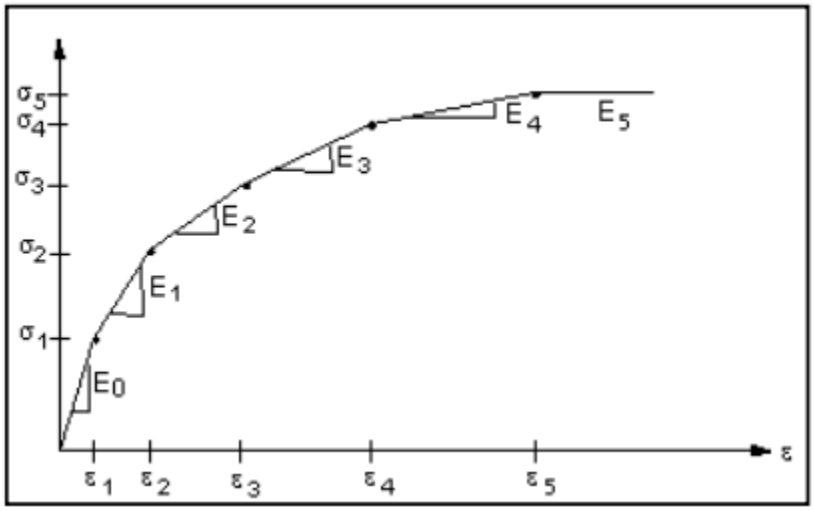

Figure 2.12. Uniaxial stress-strain curve for Multi-linear Isotropic Hardening (ANSYS, 2007)

He calculates the dilation angle from the volumetric and axial strain measurement in the monotonic triaxial tests. According to the triaxial test results analysis, the dilation angle (ψ) he obtained is 33^0 , $\psi = 0.58$ in radians. Apart from these parameters the other ballast parameters he used for simulation were based on the triaxial test results. The initial density of ballast was 1540 kg/m3, the Poisson υ ratio was 0.3.

2.6. Factors influencing the deterioration of railway Tracks

2.6.1. Stress Level

The stress level is one of the most important factors affecting the development of permanent deformation in granular materials. Selig and Waters (1994) indicated that the permanent strain of ballast was a function of both the confining pressure and the cyclic deviator stress. Knutson (1976) concluded that permanent strain accumulated after a certain number of repeated loads was directly related to the ratio of deviator stress to confining stress, as shown in Figure 2.13.

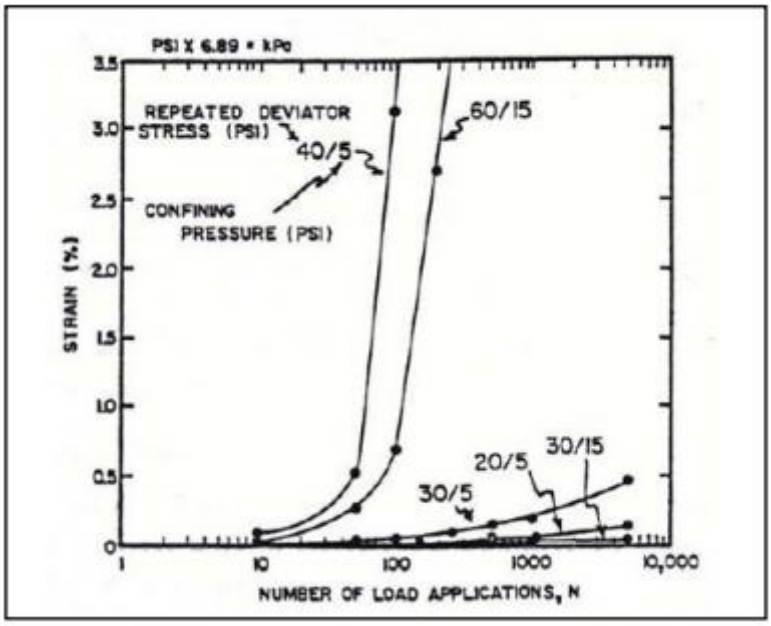

Figure 2.13. The effect of stress ratio on permanent strain (Knutson, 1976)

Clearly, confining pressure and the cyclic deviator stress have a significant effect on permanent strain accumulation. Lower confining pressure and higher repeated deviator stresses lead to a higher plastic strain over a given number of cycles. Brown (1974) conducted triaxial tests on

crushed granite and ascertained that the permanent axial strain increased with decreasing confining pressure.

The amplitude of the applied deviator stress has a significant influence on the permanent deformation characteristics of granular materials under cyclic loading. Selig and Waters (1994) stated that when a specimen was subjected to multiple magnitudes of loading, the largest load had the greatest effect on the degree of settlement. ORE (1970) showed that a small number of high amplitude loads were much more important than a large number of minor loads in establishing track deterioration. Olowokere (1975) found that volumetric strain and axial strain increased with deviator stress magnitude under cyclic loading, as shown in Figure 12. 14. It shows the significant increase of volumetric strain and axial strain due to the increase of the deviator stress ratio. Stewart (1986) indicated that the permanent strain in the first cycle increased significantly when the load amplitude was increased. Furthermore, he noted that an increase in load amplitude beyond the maximum historical stress level increased the settlement immediately, and also increased the long-term cumulative strain.

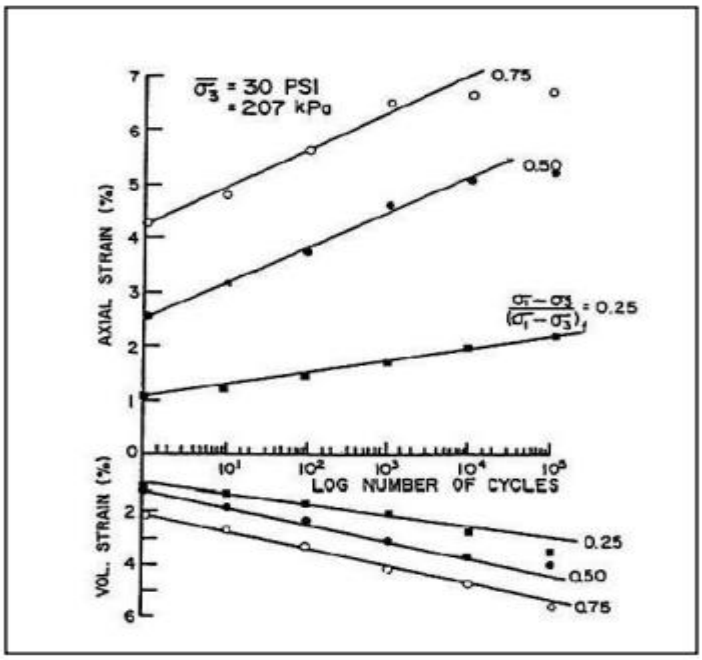

Figure 2.14. Effect of deviator stress magnitude on axial and volumetric strain (Olowokere, 1975)

2.6.2. Amplitude of Loading

The amplitude of cyclic loading plays a major role in ballast deformation. Stewart (1986) carried out a series of cyclic triaxial tests varying the load amplitude at every 1000 cycles to study the influence of load amplitude on ballast deformation and he observed that, the permanent strain in the first cycle increased significantly when the load amplitude was increased. In contrast he also concludes that, decreasing the load amplitude does not contribute to the accumulated plastic strain. In addition the final cumulative strain obtained at the end of various staged, variable-amplitude loading test (after 4000 cycles), were independent of the order of applied stresses.

2.6.3. Number of Load Cycles

Permanent deformation in granular materials under repeated loading is accumulated over an increasing number of load cycles. Shenton (1975) reported that track settlement immediately after tamping increased at a decreasing rate with the number of axles (Figure 2.15(a)). Additionally, he pointed out that the track settlement might be approximated by a linear relationship with the logarithm of load cycles (Figure 2.15(b)). The observation that settlement or vertical strain accumulated approximately logarithmically with the number of load cycles was also reported by other researchers (e.g. Raymond and Williams, 1978; Brown and Selig, 1991; Raymond and Bathurst, 1994; Selig and Waters, 1994).

Various researchers (Jeffs and Marich 1987, Ionescu et al. 1998) concluded that the permanent deformation of ballast could be characterized by two phases. The first phase was the initial consolidation where the ballast was compressed to a higher density and rapid settlement occurred. In the second phase the settlement was slower and there was an approximately linear relationship between the settlement and the number of load applications. However, according to Lekarp (1997) and Lekarp and Dawson (1998), the achievement of stable behaviour, when permanent strain rate decreases with increasing number of loading cycles, could only occur when the applied stresses were low. In contrast, higher stresses would result in a continuous increase of permanent strain.

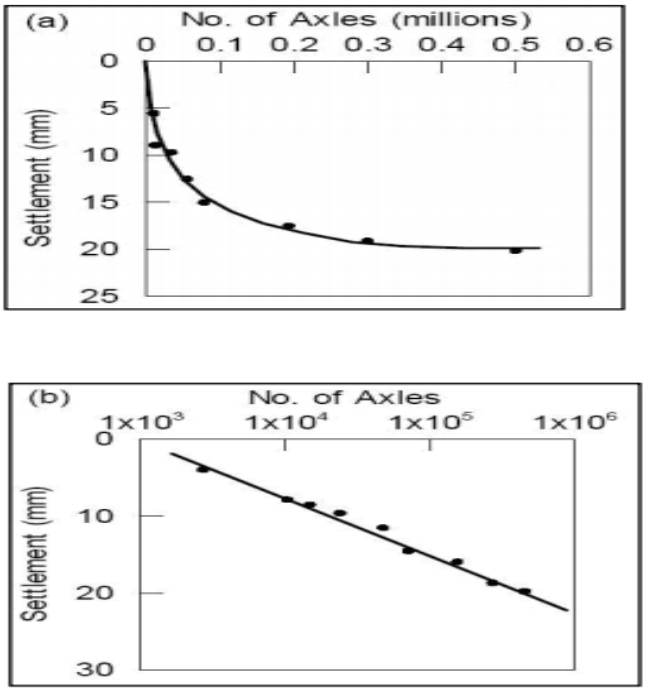

Figure 2.15 Settlement of track after tamping (a) on plain scale,
(b) on semi-logarithmic scale (Shenton, 1975)

2.6.4. Frequency of loading

Since the vehicle speed is vary with time, it is important to study the influence of loading frequency on the ballast behavior. Shenton (1975) carried out a series of cyclic loading tests, varying the frequency from 0.1 to 30Hz, while maintaining other variables (e.g. confining pressure, load amplitude etc.) constant. And he concludes that the frequency of loading does not significantly influence the deformation behavior of ballast.

CHAPTER THREE: - BALLAST DEFORMATION MODELING TECHNIQUE

3.1. Introduction

Ballast material is a collection of distinct particles which displace relative to each other, and forces between particles only exist when there is a contact between particles. These discrete characteristics of ballast materials lead to a tremendous amount of complex behavior, much of which has not yet been satisfactorily understood. The mechanical behavior of ballast material could be investigated by the discrete element method (DEM) both microscopically and macroscopically. Furthermore, the DEM has the advantage that it enables the investigation of some features which are not easily measured in laboratory tests, such as inter particle friction, distribution of contact forces, coordination number and particle movement. Although DEM provides a detailed advanced simulation, it is much more time consuming compared with the finite element method (FEM). FEM provides an alternative way to simulate ballast material deformation behavior and stress distribution.

FEM analysis has been widely used as one of the most versatile numerical techniques for engineering analysis. It can be applied to solve problems in solid mechanics, fluid mechanics, heat transfer and vibrations. In the FEM analysis, the model domain is divided into a finite number of elements. In solid models, displacements in each element are directly related to the nodal displacements, which connect each element. The nodal displacements are then related to the strains and the stresses in the elements. FEM tries to arrive at the nodal displacements, so that the stresses are in equilibrium with the applied loads. Once the equations are solved, the actual strains and stresses in all the elements can be found.

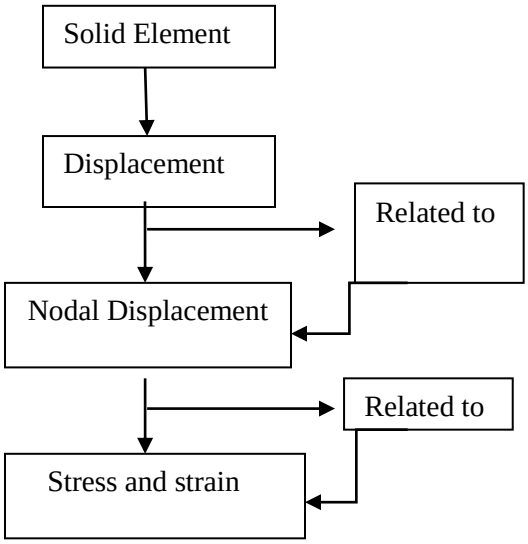

Figure 3.1. General flow chart of the Model

The main limitation of FEM analysis of ballast material is to choose a material model, which can accurately capture the material mechanical behavior. Hence, we use FEM analysis of granular materials since it should take into account the nonlinear stress-strain relationship.

In this paper, the commercial finite element analysis application ABAQUS Version 6.12.1 was used. Similar to other general, commercial finite element packages, the Abaqus program has many computing capabilities, ranging from a simple, linear, static analysis to a complex, nonlinear, transient dynamic analysis. The user's manual of Abaqus indicates that this program is a general-purpose program, which can be used for almost any type of finite element analysis in virtually any industry such as automobiles, aerospace, railways, etc. In ABAQUS Version 6.12.1, the extended Drucker-Prager model is available to model frictional materials, which are typically granular like soils and rock, and exhibit stress-dependent yield (i.e. the material becomes stronger

as the stress increases). Furthermore, and also applicable to model materials in which the tensile and compressive yield strengths are significantly different.

3.2. MODELING TECHNIQUES

3.2.1. Elasto plastic Material Models

Most common engineering materials exhibit a linear stress-strain relationship up to a stress level known as proportional limit. Plastic behavior happens when stress exceeds a yield point. Beyond this limit, the stress-strain relationship will become nonlinear, where materials undergo significant increase in strain for very small increase in stress. Such increase in strain is termed plastic flow of the material. Additionally, nonlinear stress-strain relationships in an elastoplastic model can cause changes of material stiffness at different load levels.

In an elastoplastic material, the total strain of a material is considered as the sum of recoverable elastic strain and permanent plastic strain components, expressed as:

$$d\varepsilon_{ij} = d\varepsilon^{e}_{ij} + d\varepsilon^{p}_{ij} \qquad \text{(Equation 3.1)}$$

Where $d\varepsilon^{e}_{ij}$ = elastic strain increment and $d\varepsilon^{p}_{ij}$ = plastic strain increment.

The numerical functions that define a material behavior at the yield limit are termed yield functions or yield criteria.

The elasto plastic material behavior after yielding can be defined as perfectly plastic, strain hardening or strain softening plasticity. Chen (1994) indicated that both Mohr-Coulomb and Drucker-Prager criteria satisfy most of the characteristic behavior of granular materials. Both criteria are commonly used for modeling granular materials.

As the figure 3.2 below shows, the material under consideration start yielding ,at appoint of proportional limit, may harden along the yield line and become zero after certain plastic strain occur during unloading. A new process after unloading shows the hardening process after first plastic strain developed from initial plastic strain and continues with the same hardening curves.

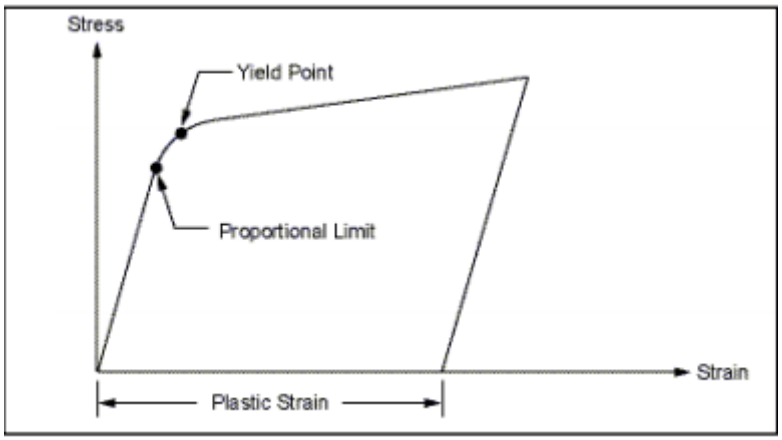

Figure 3.2. Elastoplastic stress-strain curves (ANSYS, 2007)

3.2.2. Drucker-Prager Model

The Drucker-Prager model is an elasto plastic model based on either associated or non associated flow rules. The yield surface does not change with progressive yielding, hence there is no hardening rule and the material is elastic-perfectly plastic. This criterion can be defined as a yield surface (Fs) in a p'-q stress space given by Equation 3.20 and shown in Figure 3.3. The failure surface in 3D space of principal stresses is simplified to a cone, as shown in Figure 3.4.

$F_s = q - p'\tan\beta - d = 0$ ---------- (Equation 3.2)

Where:- q = principal stress difference.

P' = Mean effective stress

β = the angle of the yield surface in p' – q stress space.

d = the intercept of the yield surface in p' – q stress space.

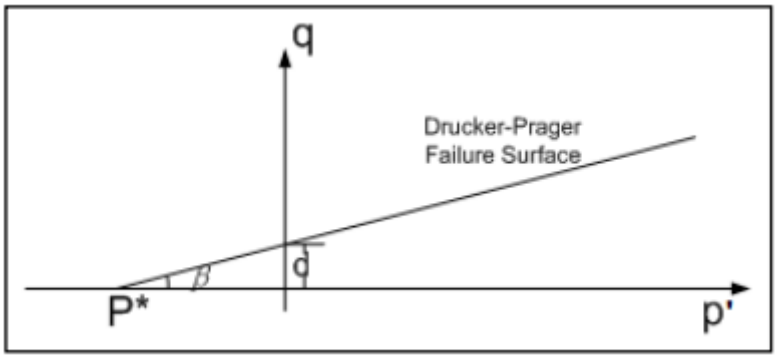

Figure 3.3 Drucker-Prager yield surface in 2D p'-q stress space

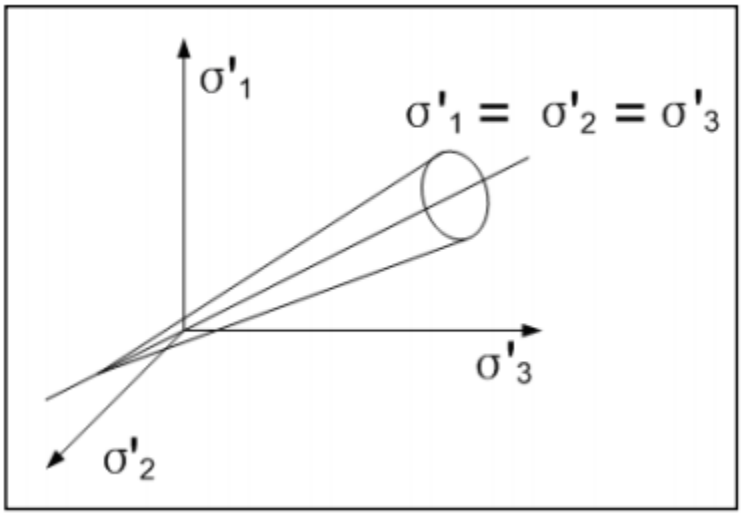

Figure 3.4 View of Drucker-Prager failure surface in 3D space of principal stresses

3.2.3. Extended Drucker-Prager Model

The extended Drucker-Prager models are used to model frictional materials, which are typically granular-like soils and rock, and exhibit pressure-dependent yield (the material becomes stronger as the pressure increases).

The extended Drucker-Prager model with hardening can capture the mechanical behavior of granular materials better than the Drucker-Prager models. In Abaqus version 6.12.1, three yield

criteria are provided in this set of models. They offer differently shaped yield surfaces in the meridional plane (i.e. p'–q plane): a linear form, a hyperbolic form and a general exponent form. The yield surface can be changed with progressive yielding using isotropic hardening plasticity material options.

The yield function with linear form is given by Equation 3.3 and shown in Figure 3.5:

$$Fs = q + \alpha p' - \sigma_y(\varepsilon_{pl}) = 0 \qquad \text{(Equation 3.3)}$$

where, α = material parameter referred to as pressure sensitive parameter,

$q = [\frac{3}{2}\{S\}\{S\}^T[M]\{S\}]^{\frac{1}{2}}$, $\{S\}$ = deviator stress vector

$\sigma_y(\varepsilon_{pl})$ = Yield stress of material

p' = mean effective stress $= \frac{1}{3} * (\sigma x' + \sigma y' + \sigma z')$

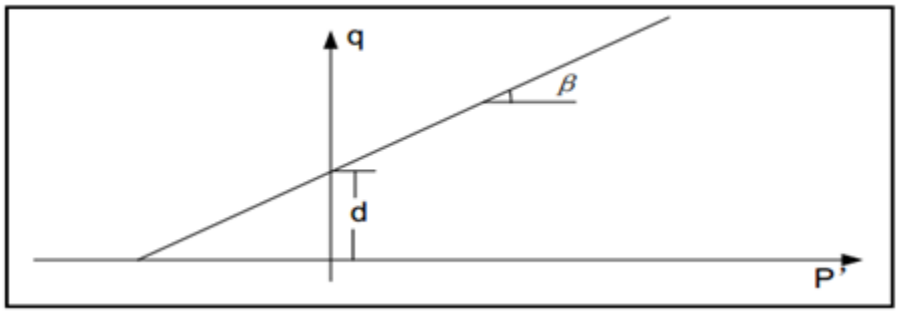

Figure 3.5 Linear Drucker-Prager yield surfaces in the meridional plane

The relationship between plastic strain ratio and stress ratio is termed the flow rule governing the mechanism of plastic deformation. The flow rule defines the subsequent increment of the plastic strain of a yielding body subjected to further loading. This is established through the concept of flow potential Q, which defines the direction of plastic strain increment given by:

$$\varepsilon_{pl} = \lambda \frac{\partial Q}{\partial \sigma} \qquad \text{(Equation 3.4)}$$

where λ= plastic multiplier, that depends on the state of stress and load history.

If the potential and yield functions coincide with each other, the flow rule is called the associated flow rule. Otherwise, the non-associated flow rule applies. As the associated flow rule is utilized in the extended Drucker-Prager material model in Abaqus, the flow potential Q for linear form is defined as:

$$Q = q + \alpha p' - \sigma_y(\varepsilon_{pl}) \qquad \text{(Equation 3.5)}$$

The hardening rule describes the changing of the yield surface with progressive yielding, so that the stress states for subsequent yielding can be established. Isotropic hardening is utilised in the extended Drucker-Prager model in Abaqus. In isotropic hardening, the yield surface remains centred about its initial centerline and expand in size as the plastic strains develop. Figure 3.6 (a) shows isotropic work hardening in the $\sigma_1' - \sigma_2'$ plane and Figure 3.6 (b) shows hardening in the p'-q plane.

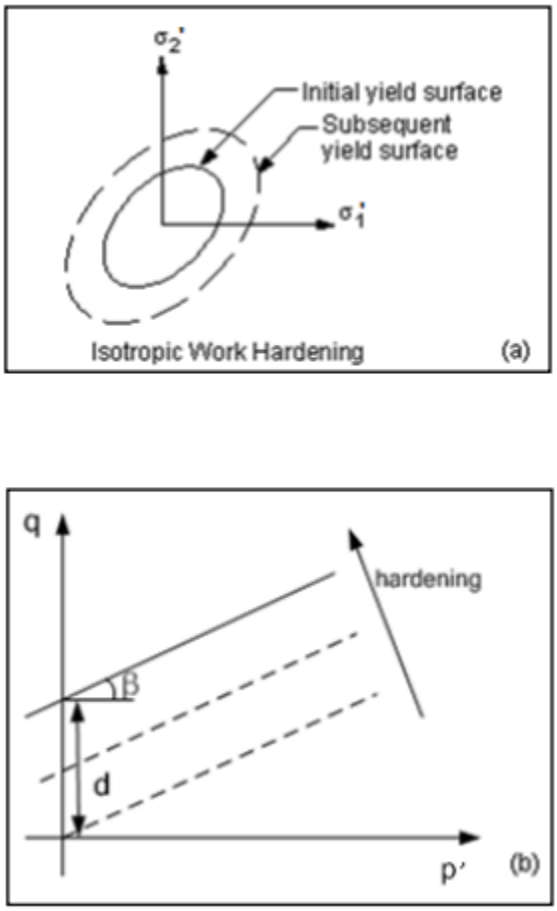

Figure 3.6. Isotropic hardening in (a) σ1- σ 2 plane, (b) p'-q plane

The choice of model depends largely on the analysis type, the kind of material, the experimental data available for calibration of the model parameter and the range of stress values that the material is likely to experience. However, the linear model is intended primarily for applications where the stresses are for the most part compressive. Hence, we used an extended Drucker-Prager model with linear yield criterion to simulate railway ballast deformation and stress conditions in this research.

The input parameters for extended Drucker-Prager models can be obtained by matching experimental triaxial test data. In the triaxial test, the specimen is confined by a compressive

stress, which is held constant during the test. The loading is an additional tension or compression stress applied in one direction. However, due to lack of trail axial test machine the input parameters used in this paper were assumed to be similar with the data observed in the literatures. And the inaccuracy of the analysis result can be expected since the materials used in the literature may not represent the actual materials at the study cases. For the sake of simplicity the summary of data adopted from the literature is tabulated as follows in table: 3.1.

Table 3.1. Summary of data adopted from literature while using extended Drucker-Prager models as elastic and plastic property of materials

Parameters	Values	Unit
Density of ballast (ρ)	1540	Kg/m3
Friction angle of ballast (Ø)	55	Degree
Dilation angle (ψ)	33	Degree
Poisson's ratio (υ)	0.3	-
Elastic modulus (E)	120	Mpa

3.3. **Plasticity theories**

Most materials of engineering interest initially respond elastically. Elastic behavior means that the deformation is fully recoverable: when the load is removed, the specimen returns to its original shape. If the load exceeds some limit (the "yield load"), the deformation is no longer fully recoverable. Some part of the deformation will remain when the load is removed.

Plasticity theories model the material's mechanical response as it undergoes such non recoverable deformation in a ductile fashion. The theories have been developed most intensively for metals, but they are also applied to soils, concrete, rock, ice, crushable foam, and so on.

Most of the plasticity models in Abaqus are "incremental" theories in which the mechanical strain rate is decomposed into an elastic part and a plastic (inelastic) part.

3.4. Elastic response

The Abaqus plasticity models also need an elasticity definition to deal with the recoverable part of the strain. In Abaqus the elasticity is defined by including linear elastic behavior or, if relevant for some plasticity models, porous elastic behavior in the same material definition.

When performing an elastic-plastic analysis at finite strains, Abaqus assumes that the plastic strains dominate the deformation and that the elastic strains are small. This restriction is imposed by the elasticity models that Abacus uses.

In Abaqus/Explicit the elastic strain energy reported is updated incrementally. The incremental change in elastic strain energy ($\Delta \varepsilon e$) is computed as , $\Delta Ee = \Delta Et - \Delta Ep$ where ΔEt is the incremental change in total strain energy and ΔEp is the incremental change in plastic energy dissipation. ΔEe is much smaller than ΔEt and ΔEp for increments in which the deformation is almost all plastic.

3.5. Specifying initial equivalent plastic strains (PEEQ) of ballast Materials

Initial values of equivalent plastic strain can be specified in Abaqus for elements that use Drucker-Prager plasticity ("Extended Drucker-Prager models,") by defining initial hardening conditions. The equivalent plastic strain (output variable PEEQ) then contains the initial value of equivalent plastic strain plus any additional equivalent plastic strain due to plastic straining during the analysis. However, the plastic strain tensor (output variable PE) contains only the amount of straining due to deformation during the analysis.

The simple one-dimensional example shown in Figure 3.7 illustrates the concept. The material is in an annealed configuration at point A; its yield stress is σ^o_B . It is then hardened by loading it along the path (A,B,C,D) ; the new yield stress is σ^o_E . A new analysis that employs the same hardening curve as the first analysis takes this material along the path (D,E,F) , starting from point D, by specifying a total strain ε_2, . Plastic strain ε^{pl}_2will result and can be output (for instance) using output variable PE11.

To obtain the correct yield stress, σ^o_E, the equivalent plastic strain at point E,ε^{pl}_1 , should be provided as an initial condition. Likewise, the correct yield stress at point F is obtained from an equivalent plastic strain PEEQ = $\varepsilon^{pl}_1 + \varepsilon^{pl}_2$

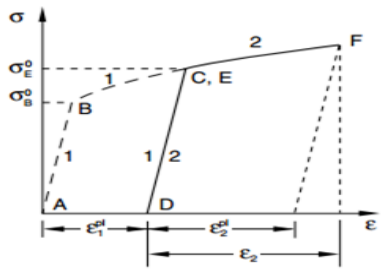

Figure 3.7.Initial equivalent plastic strain

3.5.1. Extended Drucker-Prager plasticity model for ballast

The extended Drucker-Prager family of plasticity models describes the behavior of granular materials or polymers in which the yield behavior depends on the equivalent pressure stress. The inelastic deformation may sometimes be associated with frictional mechanisms such as sliding of particles across each other.

This class of models provides a choice of three different yield criteria. The differences in criteria are based on the shape of the yield surface in the meridional plane, which can be a linear form, a hyperbolic form, or a general exponent form.

3.5.2. Hardening and rate dependence

For granular materials these models are often used as a failure surface, in the sense that the material can exhibit unlimited flow when the stress reaches yield. This behavior is called perfect plasticity. The models are also provided with isotropic hardening. In this case plastic flow causes the yield surface to change size uniformly with respect to all stress directions. This hardening model is useful for cases involving gross plastic straining or in which the straining at each point is essentially in the same direction in strain space throughout the analysis. Although the model is referred to as an isotropic “hardening “model, strain softening, or hardening followed by softening, can be defined. As strain rates increase, many materials show an increase in their yield strength. The effect is generally not as important in granular materials. The evolution of the yield surface with plastic deformation is described in terms of the equivalent stress, which can be

chosen as either the uniaxial compression yield stress, the uniaxial tension yield stress, or the shear (cohesion) yield stress:

We consider the stress strain data adopted from the literature and we determined the initail yield stress and plastic strain value for our modeling and it is tabulated as shown in table 3.2.

Table 3.2 Table that show the yield stress and plastic strain of ballast materials

Yield stress	Plastic strain,(%)
18887.5	0
35500	0.008
48000	0.02
61750	0.04
70875	0.06
81125	0.09
85375	0.15

CHAPTER FOUR: - FINITE ELEMENT MODELLING AND ANALYSIS

4.1. Introduction to finite element methods

Finite element method (FEM) is one of the most versatile numerical techniques for engineering analysis, as it enables a good approximation to be made even when a system exhibits non-linear material behavior. The finite element program utilized in this project is ABAQUS. It is a powerful tool and capable of analyzing a wide range of engineering problems including geomechanics. However, the FEM solution is always an approximation to the real solution, restricted by the assumptions being made in idealizing the geometry, boundary conditions and material model.

Finite element analysis has been performed to calculate the stress conditions within the ballast. Initially, an elastic material model was used to simulate a box test. The monotonic triaxial test results were then analyzed by using a Drucker-Prager material model. Furthermore, sub option, the extended Drucker-Prager material model with hardening was utilized to fit monotonic triaxial test results and calculate stress conditions within the ballast structure.

4.1.1. Modeling Procedures in ABAQUS/CAE

The ABAQUS/CAE environment is divided into different modulus, where each module defines a logical aspect of the modeling process; for instance, defining the geometry, defining the material properties, and generating a mesh. The Graphical User Interface (GUI) generates an input file with all information of the model, to be submitted to the solver, using ABAQUS/Standard or ABAQUS/Explicit routines. The solver performs the analysis and sends the information back to ABAQUS/CAE for evaluation of the results. Most models created in

ABAQUS/CAE are assembled from different parts. It always starts with creating different parts separately in the parts module. Different parts may need different material properties, which are defined in the property module. A full range of material properties are available in ABAQUS, such as elastic and plastic behavior, as well as thermal and acoustic behavior. The model then is assembled in the assembly model, by combining the different instances originates from different parts. In the step module the analysis is divided in to different analysis step, such as static and dynamic/direct cyclic analyses. These can be combined in a way to resemble the physical problem that is to be analyzed. The instances in the model will not interact with each other until they have been connected in the interaction module. The loads acting on the model are defined in the load module, as well as boundary conditions. The whole model is then meshed in the mesh module. The meshing techniques vary with the element type and the geometry of the model.

4.2. Initial Modeling

Initial modeling was carried out to investigate the ballast response with an elastic material model in a box test simulation and the ballast stress-strain behaviour with a Drucker-Prager material model in a triaxial test simulation.

4.3. Modeling Element of Ballast Material

A solid Element is considered in modeling the deterioration of ballast. Solid elements in two and three dimensions are available in ABAQUS. The two-dimensional solid element allows modeling of plane and axisymmetric problems. In three dimensions the isoparametric hexahedron element is the most common, but in some cases complex geometry may acquires tetrahedron elements. Those elements are generally only recommended to fill in awkward parts of mesh. ABAQUS provides both first-order linear and second-order quadratic interpolation of the solid

elements. The first-order elements are essentially constant strain elements, while the second-order elements are capable of representing all possible linear strain fields and are more accurate when dealing with more complicated problems.

4.3.1. Sample Simulation for modeling

Before the analysis has been started, it needs to simulate the ballast sample used in trail axial machines based on simulation of Lim (2004) provided that simulated samples were built to represent a volume of ballast below a section of sleeper underneath the rail seat. And the sample of ballast having 300mm depth with over burden crib depth of 150mm at either sides of 150mm depth of sleeper have been considered in order to take the ballast materials under real situations.

Besides, since the properties of ballast materials under cyclic loading is vary at different depths of ballast layers due to consolidation and compaction during the ballast installation 300mm thick solid sample of ballast had been categorized into three layers to consider the properties of ballast samples at different 100mm intervals below the sleeper.

4.4. Vertical loading simulation

A moving train load causes the deterioration of ballast through the stress distribution from the rail to the sleepers and ballast. The magnitude of load to be subjected to the sleeper can be obtained by dividing half of train axle load (25/2 =12.5 ton) by the rail pad. Where the rail pad area is 0.045m2. Therefore Q = 2/3*12.5*10*100 kg/0.045m2 = 185178kg/m2 = 185.178kpa.

In this paper the effect of train load is modeled by dividing the ballast section in to different layers according to the Lim (2004) and the train cyclic load is directly subjected to the sleeper section as shown in figure 4.1.

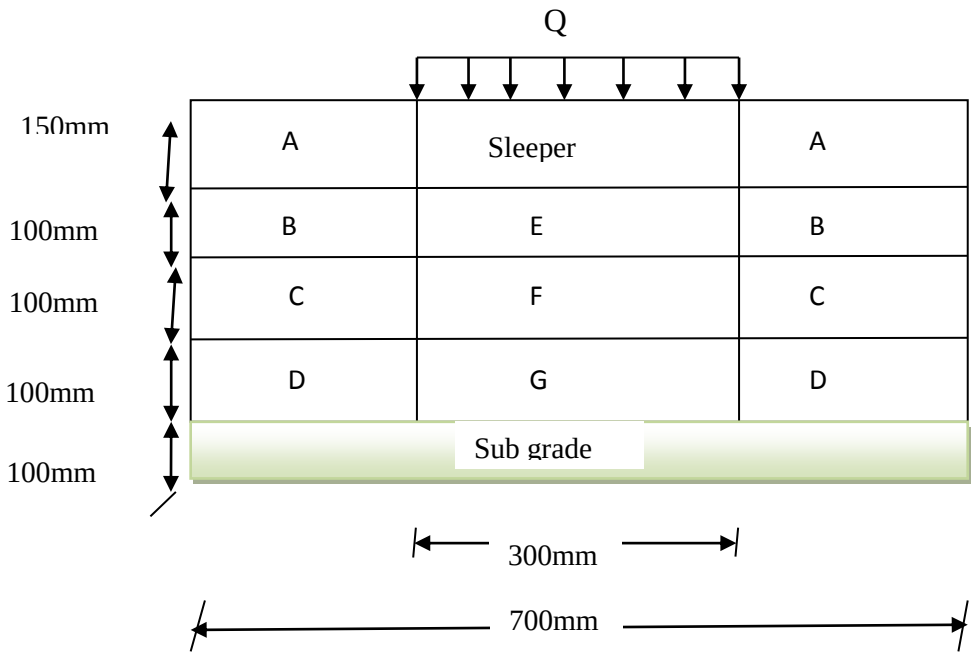

Figure: 4.1. Train cyclic load applied to the sleeper section in 2D

The model of cyclic load and boundary condition simulated using Abaqus software's can be shown as shown in figure 4.2. Where the boundary condition we used were simply supported from both sides and fixed support from the bottom.

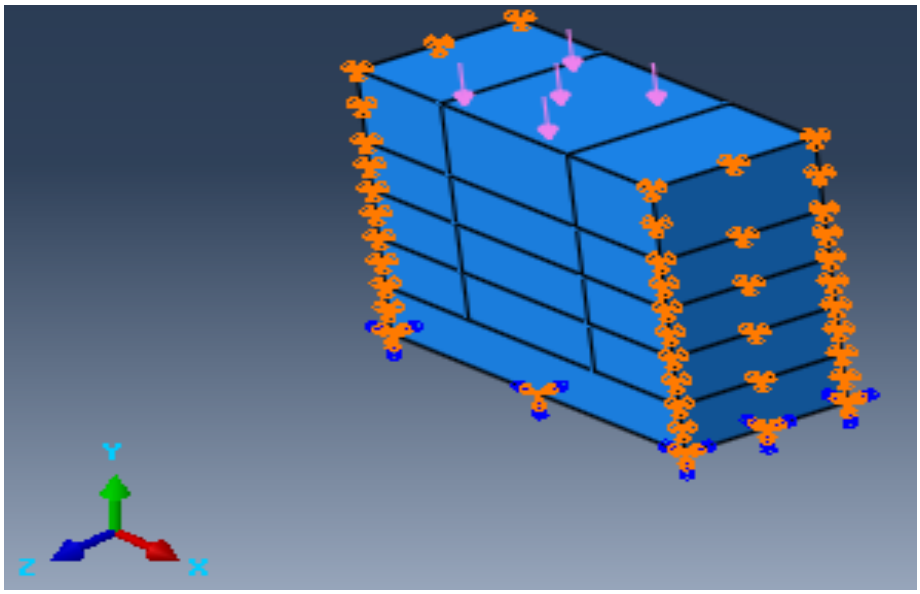

Figure: 4.2. Simulation of ballast layers and loading condition subjected to the sleeper section

4.5. Elastic Modeling

To model fully elastic behavior of ballast materials we consider solid element for simulation. Elastic material requires three physical properties that need to be applied to the test specimen which are Young's Modulus, density and Poisson's Ratio. The 3-dimensional structural model of the box test simulation and assigned material properties with an elastic model is shown in Figure 4.2 (a).

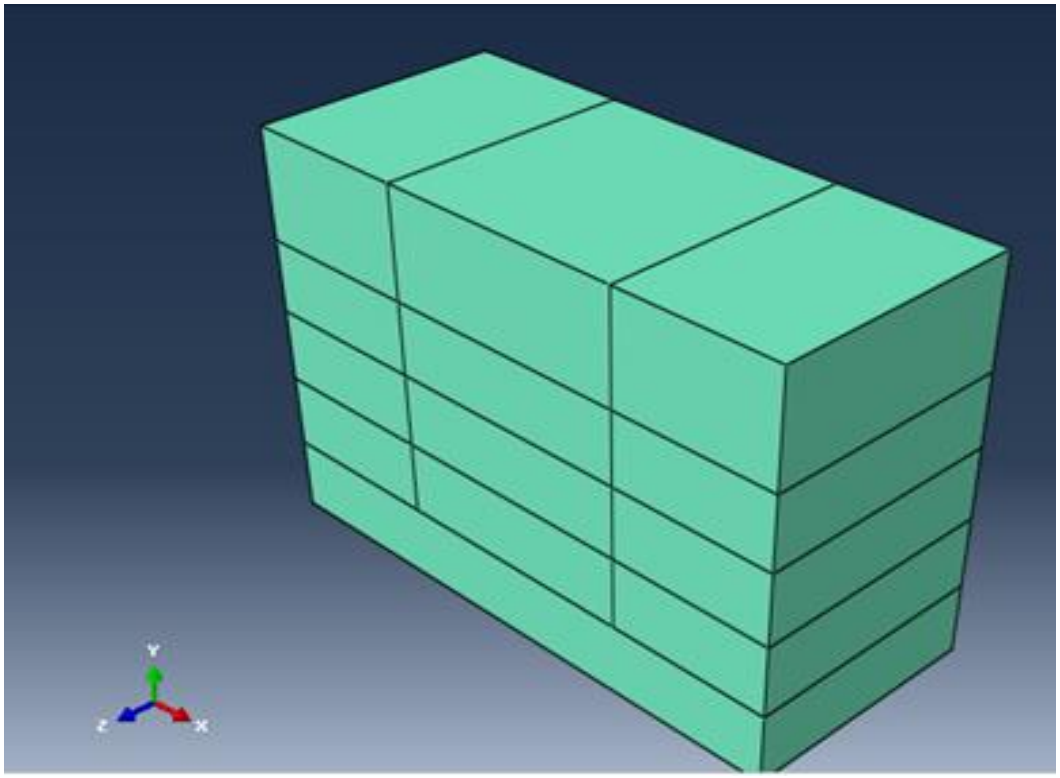

Figure 4.2 (a) Structural details of simulated layers with Assigned material property

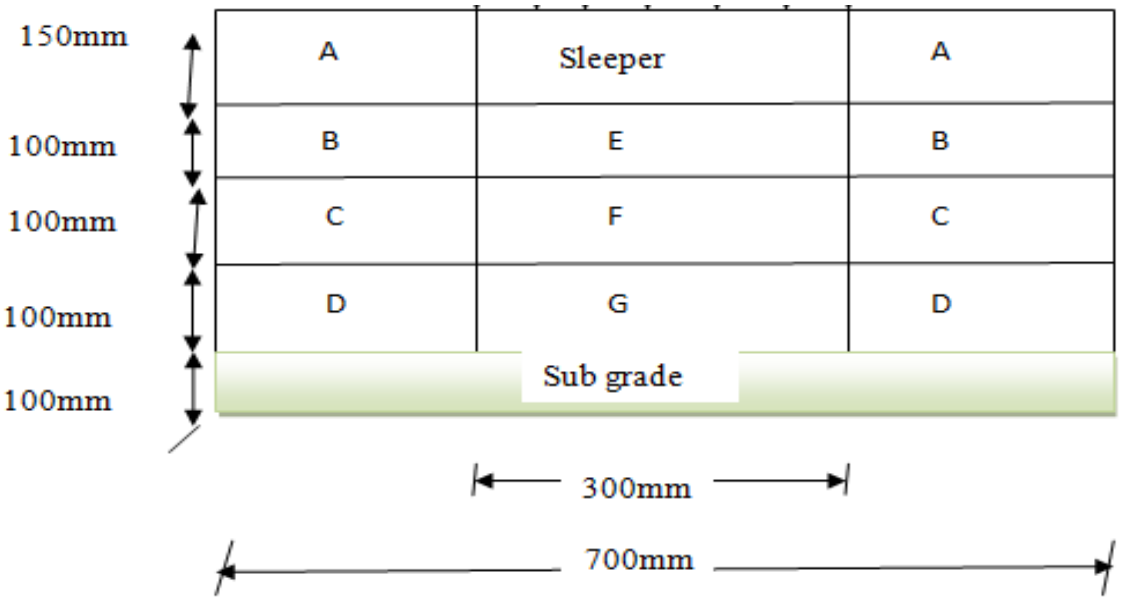

Figure 4.2 (b) Front elevations with different designation for simulated layers

Figure 4.2 (b) shows the front elevation divided into different sections with different parameters in the simulation. The ballast in different areas under or around the sleeper is assumed to have different parameters, such as density, Poisson's ratio and Young's Modules, due to consolidation and compaction during the ballast installation. Parameter details are listed in the Table 4.1. All parameters used for this paper were chosen based on the box test results by Lim (2004). The thickness of the ballast in the box test is 300mm with 150mm thick overburden crib ballast.

In actual cases different compaction methods were used for the ballast underneath the loading sleeper section and overburden crib ballast. So that behaviors of ballast material under the sleeper have different properties at different coordinates of the simulated sections. Therefore, the ballast in Section A is relatively looser than other sections and the parameters used during the modeling for each layer can be tabulated as shown in table 4.1 below. Sleeper section is simulated with

typical concrete properties used by Chiara Paderno, LAVOC – EPFL, (9th Swiss Transport research conference paper STRC 2009).

Table 4.1 Parameters used in box test elastic modeling based on Lim (2004)

Ballast Position	Density (kg/m3)	Poisson's ratio	Young's Modulus (Pa)
Section A	1700	0.35	100E6
Section B	1800	0.33	120E6
Section C	1800	0.33	120E6
Section D	1800	0.33	120E6
Section E	1800	0.33	120E6
Section F	1800	0.33	120E6
Section G	1800	0.33	120E6
Concrete Sleeper	2800	0.2	30E9
Sub grade	1770	0.3	20Mpa

In this model, 3-dimensional 8-node isoperimetric structural solid elements were used to simulate both the sleeper and the ballast material. In Abaqus, this element is named C3D8R, which is defined by eight nodes having three degrees of freedom at each node: translation in the nodal x, y and z directions. The top surface of the ballast and the sleeper had free boundary conditions. But we use the fixed and pin supports for bottom surface and both sides respectively. The simulated loading used in this paper is a monotonic load of train cyclic load with a magnitude

of 25 ton, which was the maximum assumed train load value in the cyclic loading for Ethiopian national railway projects. As this is an elastic model, there is no plastic strain produced by the loading. The results obtained after running the simulation are discussed under the chapter five.

CHAPTER FIVE: - RESULTS AND DISCUSSIONS

5.1. Elastic Result of Ballast modeling

5.1.1. Vertical Displacement of the ballast materials

The main reason for the sleeper displacement is the progressive deformation of the ballast under the sleeper and, most of all on its low external corner. The maximum displacement occurs on the external sleeper side. And it can be observed that, the first vertical displacement of ballast layer is high (i.e. around 6.7mm) at the upper layer due to the application of cyclic loading produced further compression on the ballast as shown in figure 5.1(a) below.

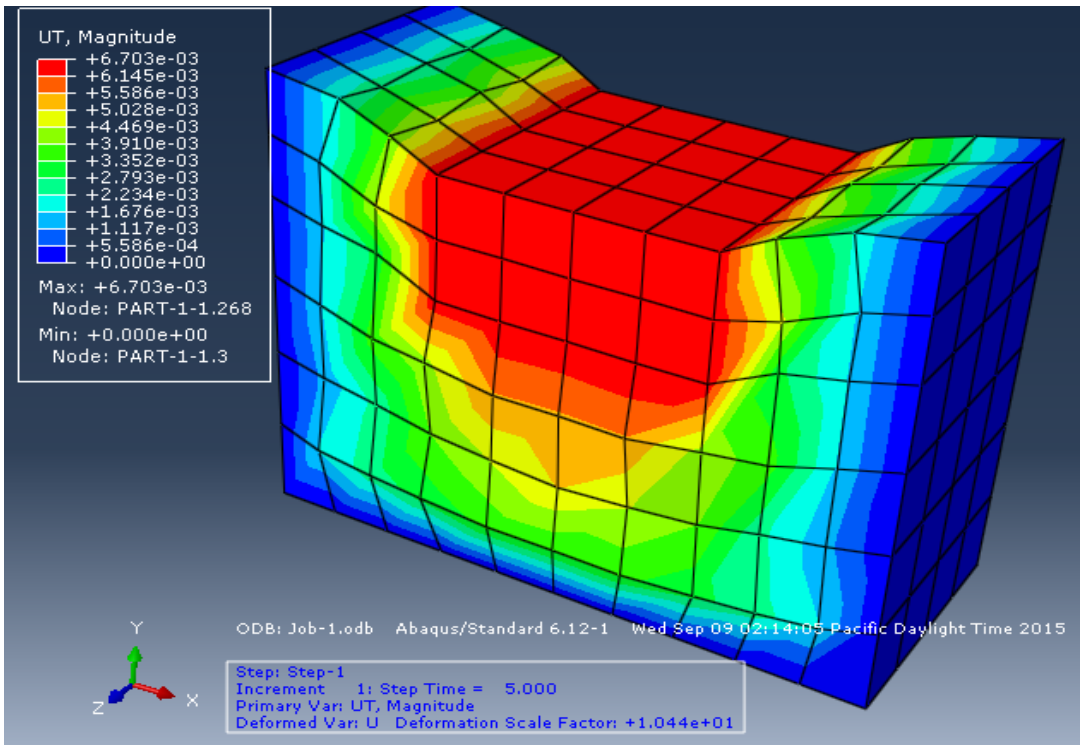

Figure 5.1 (a). Simulation of Vertical displacement (Unit: m)

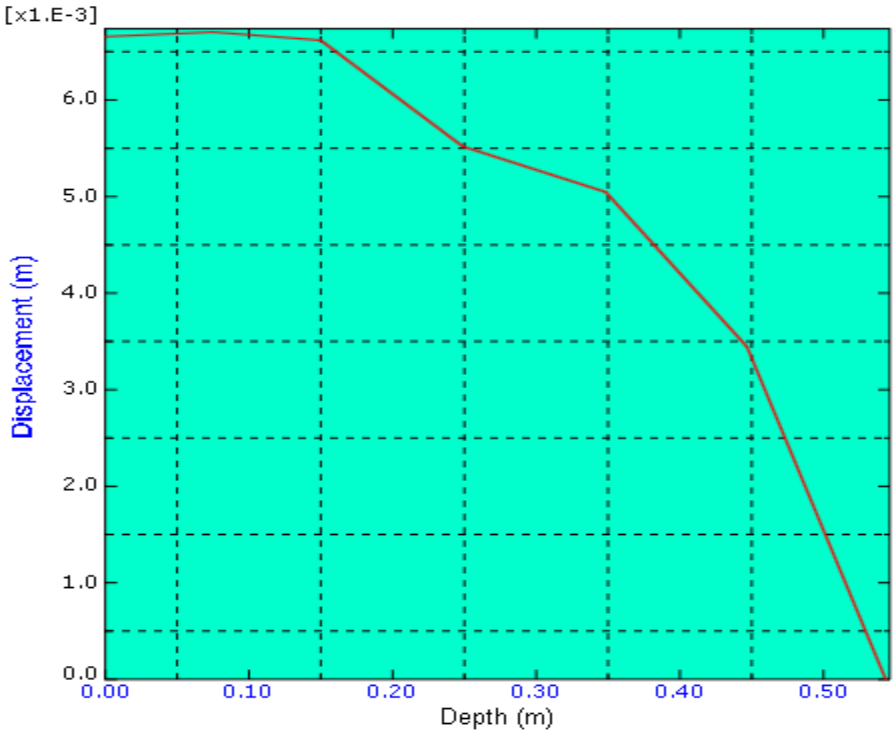

Figure 5.1 (b) Vertical displacement of ballast with depth (Unit: m)

5.1.2. Elastic Strain Distribution

The result obtained from the model to show the elastic strain distribution of the ballast materials subjected to cyclic loading indicates that it is maximum at the bottom corner of sleeper and it is vary non linearly with depths. And though the ballast is deformed elastically in staggered manner as shown in figure 5.2 (b), it can be recovered after the load is removed to its initial un deformed shape.

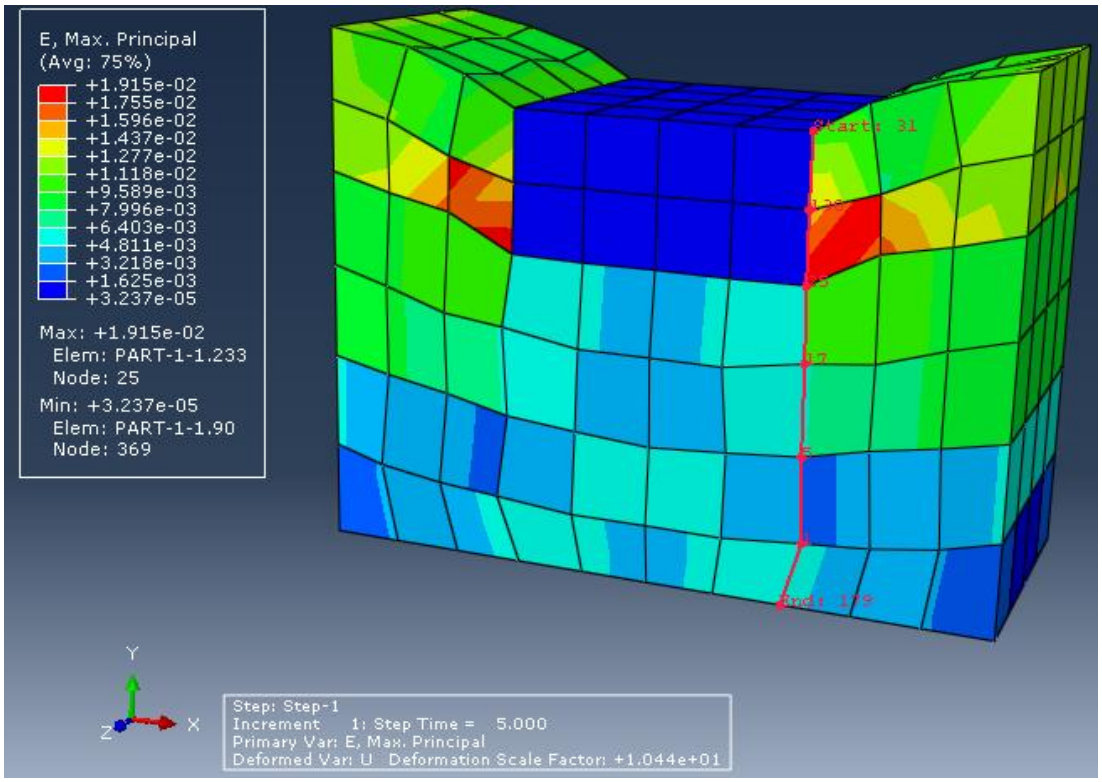

Figure 5.2(a) Elastic strain distribution Simulation

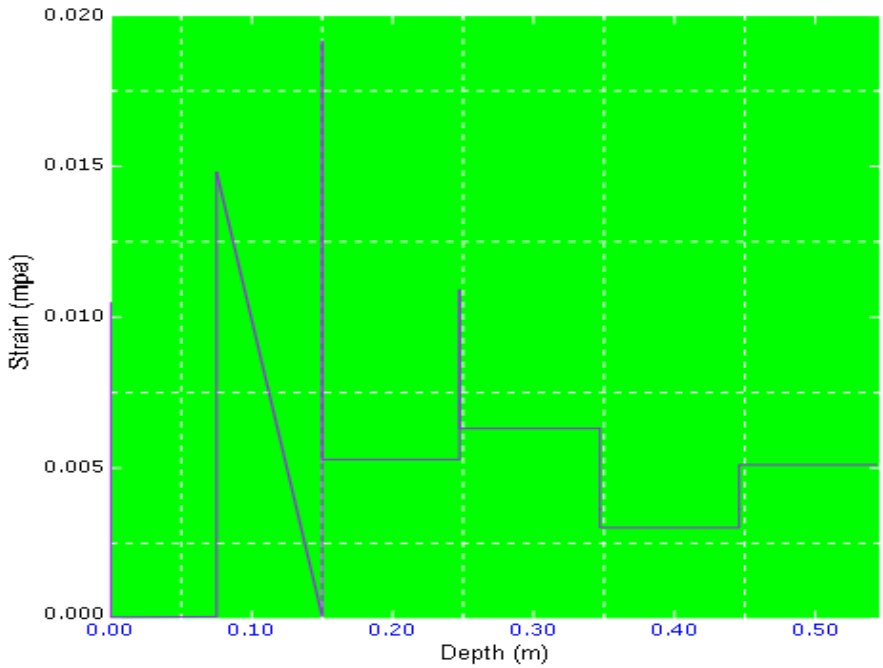

Figure: 5.2 (b) The Elastic strain distribution in the box test simulation with depth of ballast at different nodes

5.1.3. Elastic Stress Distribution

The vertical stresses results, shown in figure 5.3 (a) below, are all concentrated in the sleeper and mostly damped by the stiff concrete. The sleeper diffuses uniformly a share to the ballast bed, which dumps the residual charges by deformation. Then the stresses are propagated from the ballast to the underling infrastructure layers in a conic form.

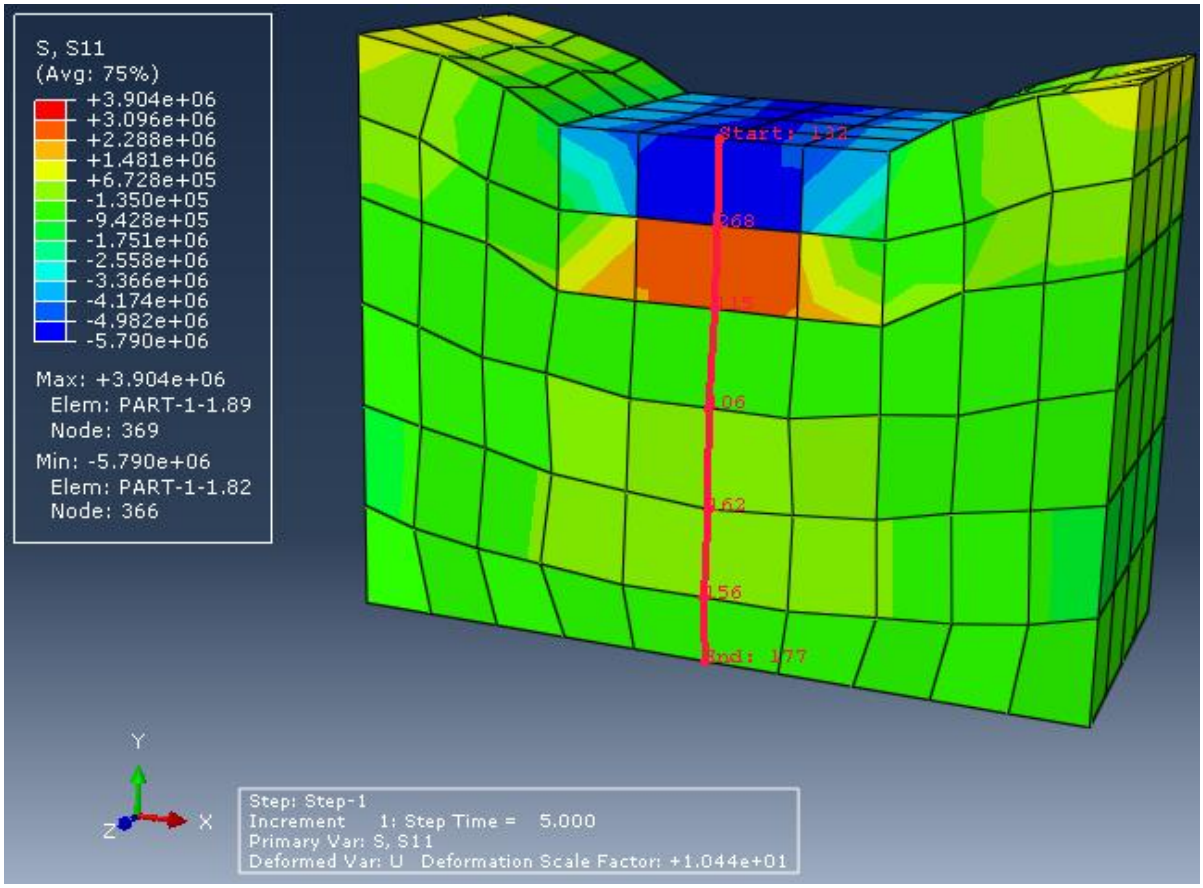

Figure: 5.3 (a) Simulation of the Elastic stress distribution

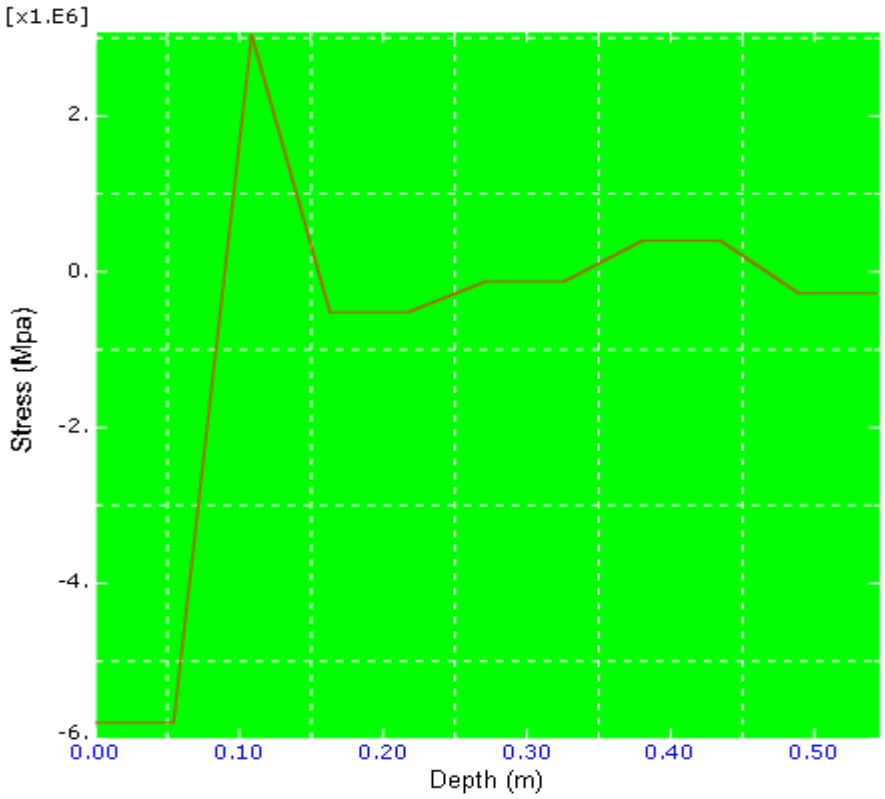

Figure: 5.3 (b) The Elastic stress distribution in the box test simulation along the path

As the figure 5.3 shows the maximum stress is induced under the bottom of the sleeper and it decreases with increasing the depth of ballast layers and increases with load repetitions.

5.2. Elasto plastic Cases of Material Modeling

To perform the elasto-plastic analysis, the elastic mechanical properties are still required because this will provide the stress-strain relationship up to the yield point but additional information is required to ensure the plastic range. To develop the plastic range in FEA, the yield stress and plastic strain data's are need to be manually loaded into the material properties.

Considering the Stress strain data reviewed in the literature, chapter two, the validation of used data in monotonic trail axial test can be checked as follows. Where reviewed data in the literature are tabulated as shown in table 5.1. And these data can be used in order to consider the hardening behavior of ballast materials during elasto plastic simulation.

Table: 5.1. Table that shows stress strain behavior of ballast under different confining pressure

Strain (%)	Stress@5kpa confining pressure(Kpa)
0	0
0.05	4.85
0.8	15
2	20
4	26
6	29.5
9	30.5
15	31.5

Strain (%)	Stress@10kpa confining pressure (kpa)
0	0
0.05	7.7
0.8	20
2	25
4	36
6	39
9	42
15	44

Strain (%)	Stress@30 kpa confining pressure(kpa)
0	0
0.05	30
0.8	46
2	55
4	77
6	85
9	91
15	92

Strain (%)	Stress@60kpa confining pressure(kpa)
0	0
0.05	33
0.8	61
2	92
4	108
6	130
9	161
15	174

To calibrate the yield parameters we need to decide which point on each stress-strain curve will be used for calibration. To calibrate the initial yield surface, the point in each stress-strain curve corresponding to initial deviation from elastic behavior should be used. Alternatively, if we wish to calibrate the ultimate yield surface, the point in each stress-strain curve corresponding to the

peak stress should be used. One stress data point from each stress-strain curve at a different level of confinement is plotted in the meridional stress plane (q–p plane). And this technique calibrates the shape and position of the yield surfaces as shown in figure 5.4.

Points chosen to define the shape and position of the initial yield surface can be obtained using the above table 5.1 and plotted as shown in figure 5.4 below. Lastly, initial yield surfaces is plotted in meridional plane as shown in figure 5.5.

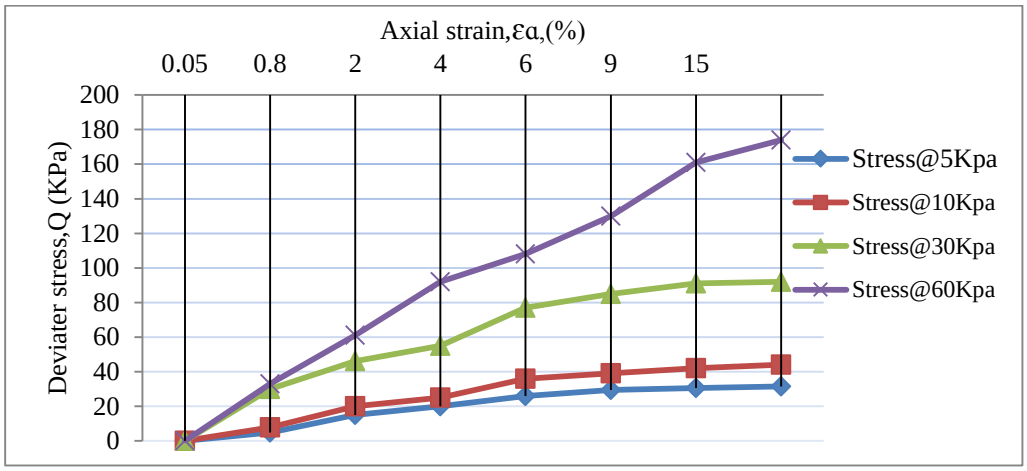

Figure: 5.4. Points chosen to define the shape and position of the initial yield surface

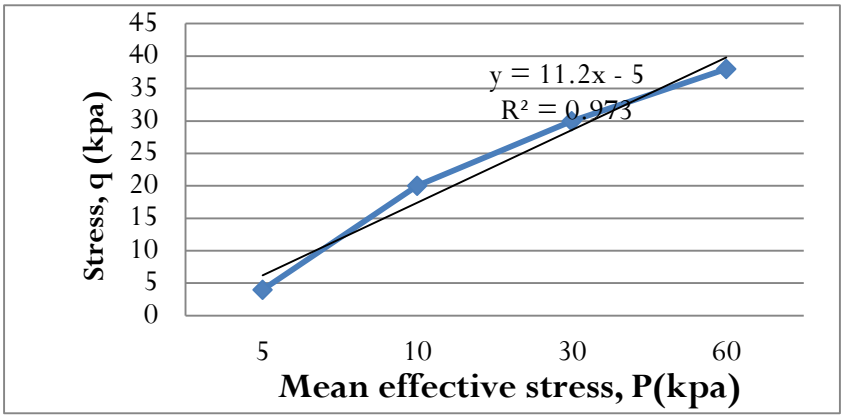

Figure 5.5. Initial yield surface plotted in the meridional plane

And from the figure 5.5, the plotted initial yield surface shows R^2 value greater than 95% which implies it is confident to use the data for modeling the ballast layers. Using stress strain data from table 5.1 and initial yield surface plotted in meridional plane from figure 5.5 above, the yield stress and Abs.plastic strain data can be calibrated.

Table 5.2. Calibrated Parameters used in extended Drucker-Prager modeling for ballast simulation in elasto plastic cases of ballast material modeling

Yield stress,(pa)	Abs.Plastic strain
18887.5	0
35500	0.008
48000	0.02
61750	0.04
70875	0.06
81125	0.09
85375	0.15

Besides, to perform elasto-plastic modeling this calibrated yield stresses and plastic strains points were manually loaded into the plastic material properties module with sub options in order to consider the hardening behavior of ballast using extended Drucker prager techniques. This is sufficient because of the small change between each stress-strain point. Note that the fully elastic material properties are also present in the material properties to ensure that stress applied up to the yield point is elastic. The way ABAQUS analyzes an elastic-plastic problem is by using the fully elastic material properties until the yield point is achieved and then it starts to apply the plastic material properties.

5.2.1. Vertical Displacement

The elasto plastic was simulated with a monotonic cyclic loading of 185.177 KN. Obtained vertical displacement is as shown in Figures 5.6 below provided that the hardening behaviors of ballast materials are included in the simulation.

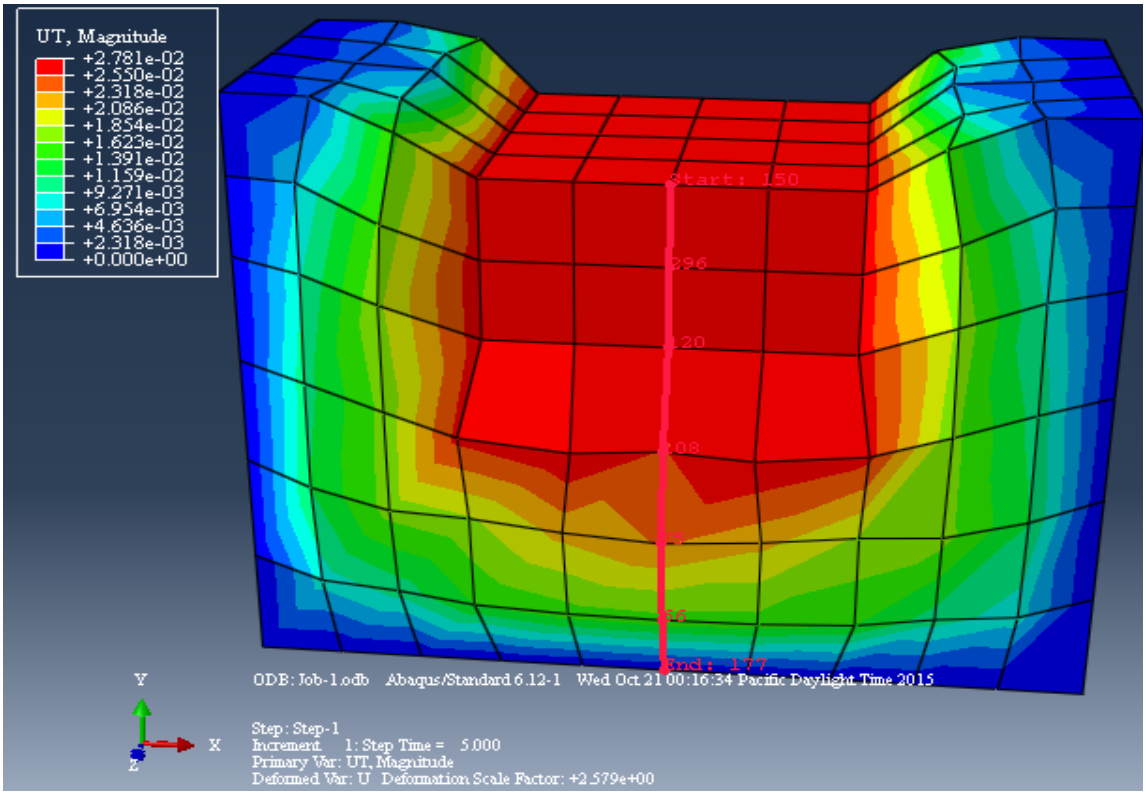

Figure 5.6. Simulation of Vertical Displacement of ballast Layer

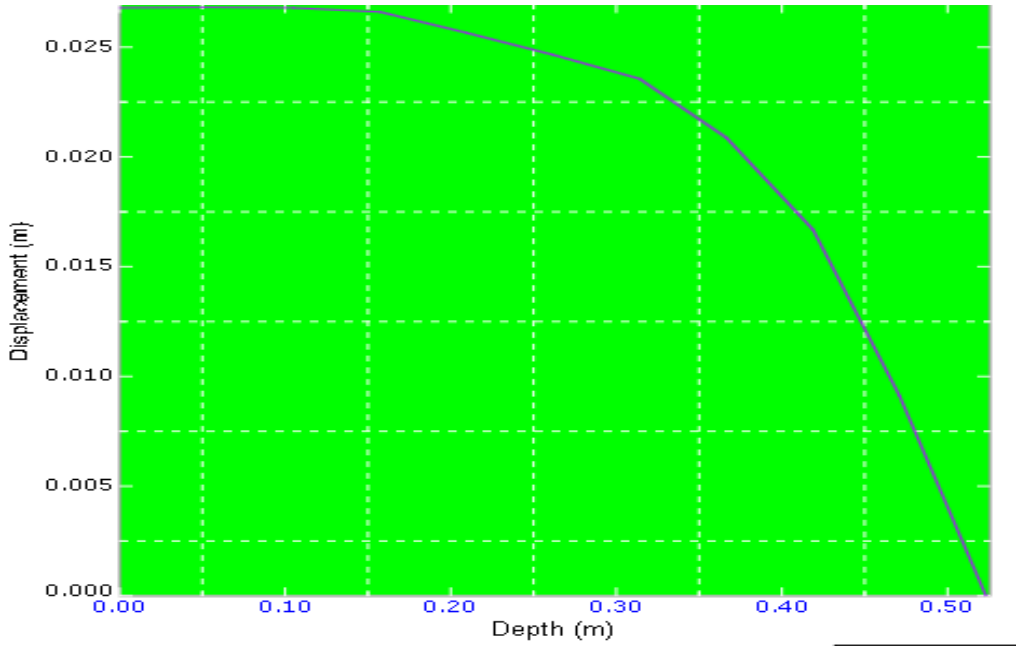

Figure 5.7. Vertical displacement of ballast with depth

As in the previous simulation of elastic case, the ballast directly underneath the sleeper has the largest settlement and it decreases from the top to the bottom. During the cyclic ballast modeling, most degradation occurs at the early stages but also accumulates with increasing number of loadings probably by particle packing in addition to the breakage of large, angular particles and it is continue decline from top to down. After particle rearrangement, further loading produced much smaller settlements. It could be postulated that new contacts were stabilized under further loading between the idle particles and the rest of specimen skeleton, and that the secondary breakage of former would then be initiated.

The maximum settlement under cyclic loading in case of elasto plastic simulation is approximately 2.781cm, which includes both the permanent and resilient settlement in the first load cycle. And it is greater than the elastic vertical deformation obtained from figure 5.1(a). (i.e. 6.703mm in case of elastic cases.)

5.2.2. Plastic Strain Distribution of Ballast

As figure 5.8 (a) shows strain concentration zones is near the sleeper corners. It appears that the ballast at the concentration zones suffers very high strain. This also highlights that the vertical strain at the two edges of sleeper are much higher than at the bottom of sleeper due to particle rearrangement during loading and particle breakage exposes a new age of ballast particle under loading.

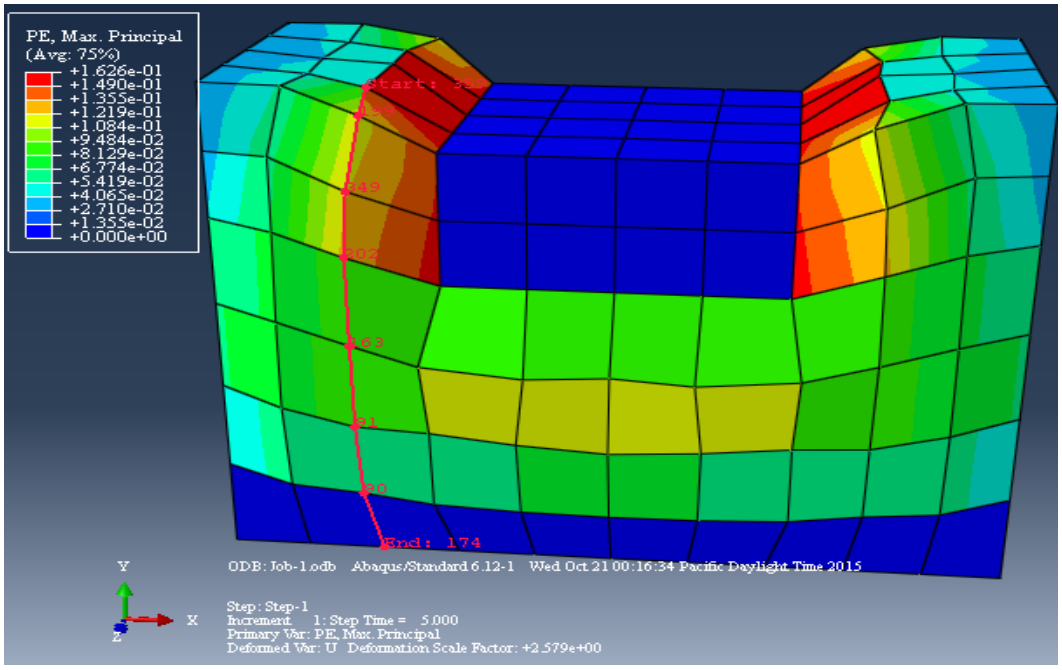

Figure: 5.8 (a) Plastic Strain Distribution Simulation

Also plastic strain distribution of ballast materials, subjected to cyclic loading, is varying non linearly with depths. And it declines from top to bottoms as shown in figure 5.8(b) below. Also the figure 5.8 indicates that ballast modeled using elasto plastic case shows more deformation than the elastic case due to limited resilient strain/elastic strain/ induced during plastic responding. Generally during the first cycle of loading on the sample the axial strain developed rapidly and it recovered only partially up on unloading. Each additional cycle caused an increment of plastic strain, but at a diminishing rate.

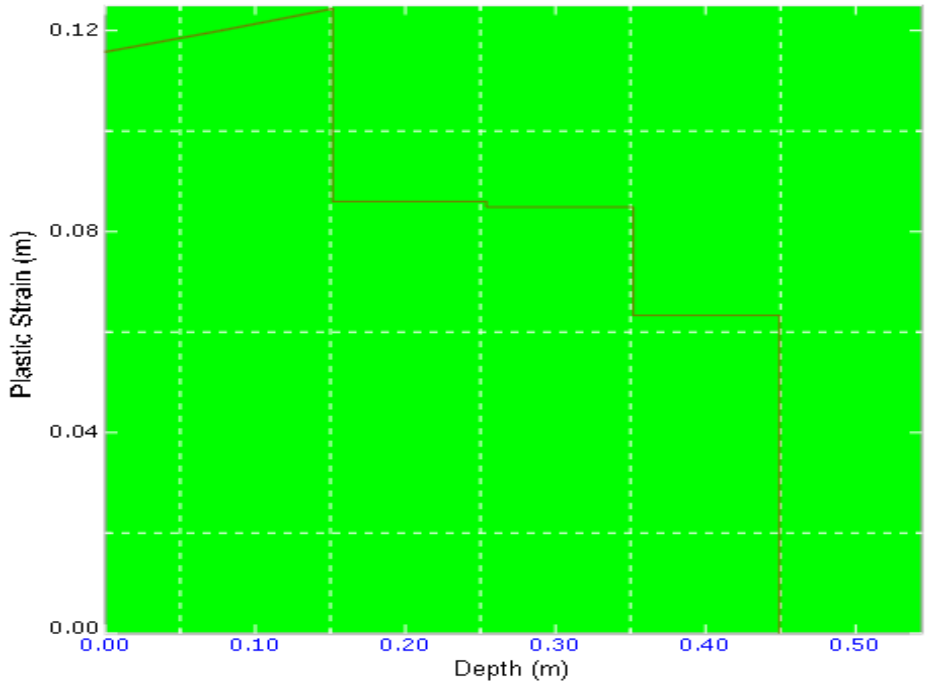

Figure 5.8(b). Plastic strain distributions along paths with depth

5.2.3. Initial equivalent plastic strains (PEEQ) of simulated ballast material

The correct initial yield stress of the ballast under investigation (i.e. σ^{o}_{E} mentioned under section 3.5) is obtained once the initial equivalent plastic strain (ε^{pl}_{1}) is determined from the

model. The model shows that initial equivalent plastic strain (PEEQ) magnitude is 11.69cm as shown in figure 5.9. And it consists of both initial value of equivalent plastic strain plus any additional equivalent plastic strain due to plastic straining during the analysis.

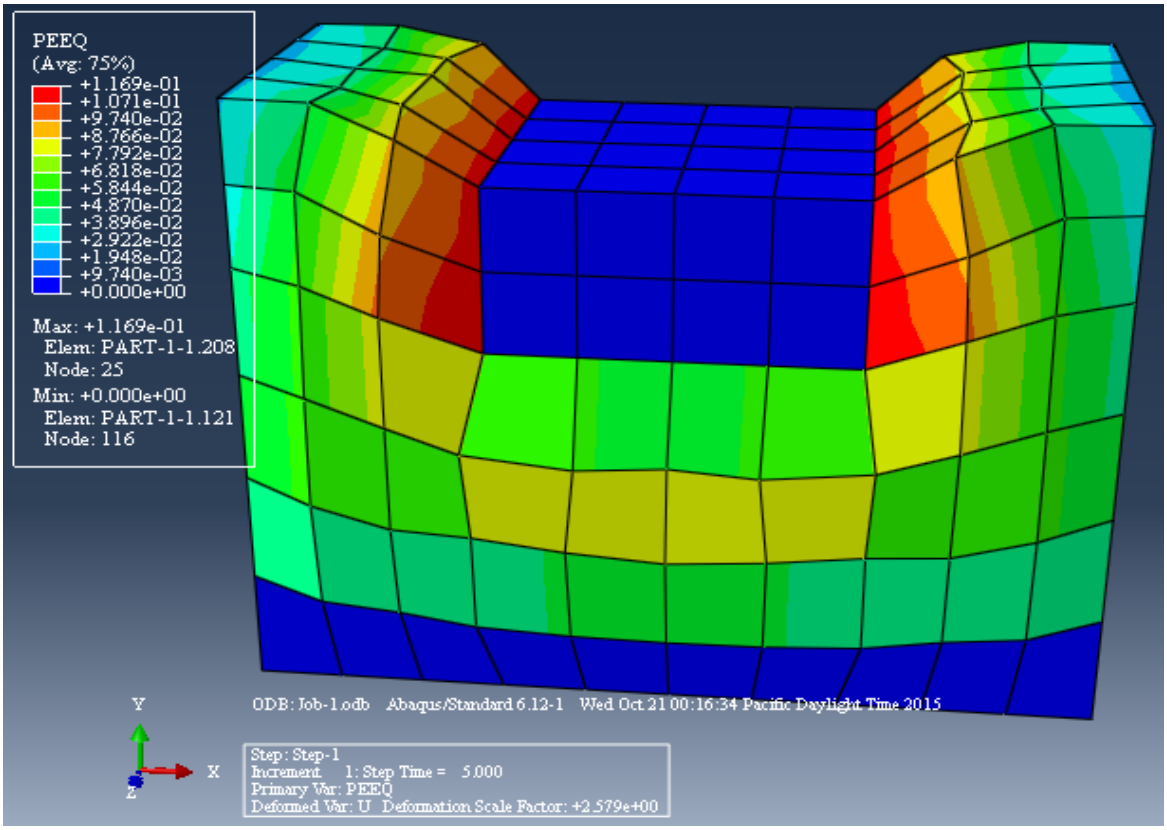

Figure.5.9. Initial equivalent plastic strain (PEEQ)

However, to determine the required yield stress it needs to now the initial equivalent plastic strain during the analysis (i.e $\varepsilon^{pl}{}_2$) and it is obtained from the output variable PE11 as shown in figure 5.10.

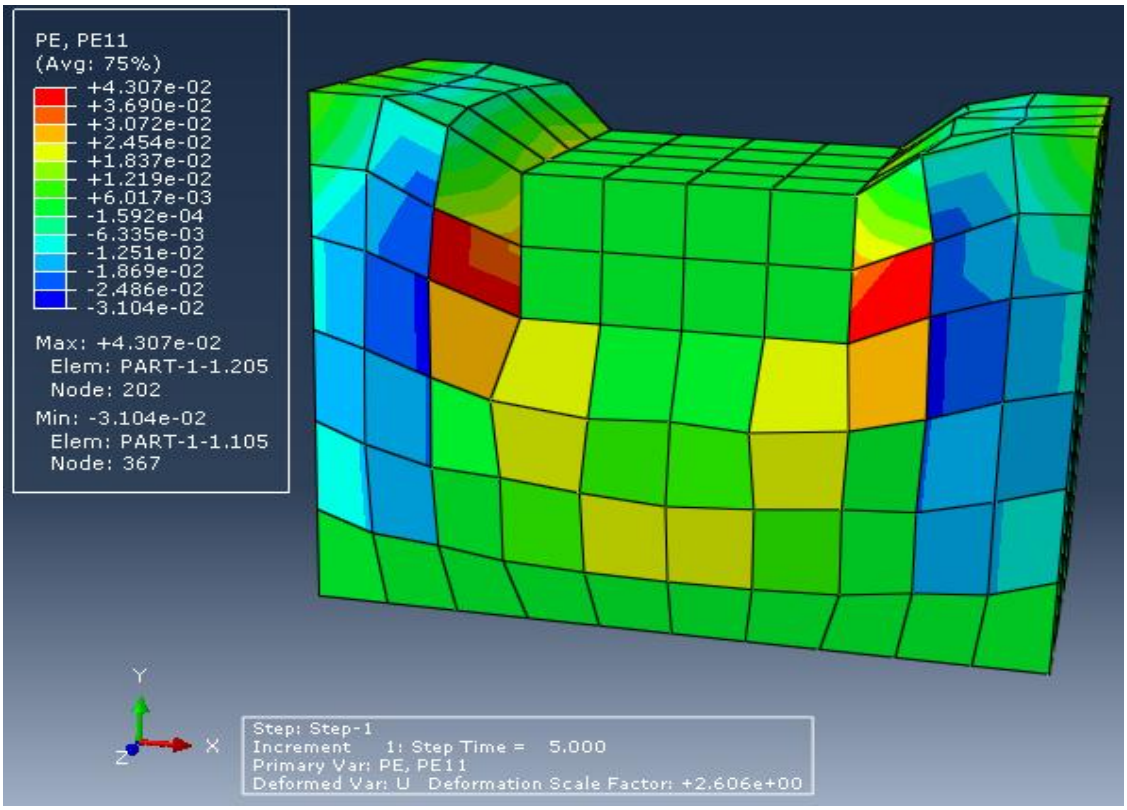

Figure 5.10. Equivalent plastic strain due to plastic straining during the analysis (ε^{pl}_2)

The figure 5.10 indicates that, the additional equivalent plastic strain due to plastic straining during the analysis (ε^{pl}_2) is 4.307cm. And, equivalent plastic strain, ε^{pl}_1, is obtained by deducting PE11 from PEEQ and it equal to 7.38 cm. Therefore, the correct plastic yield stress is determined by offsetting 7.38cm from the origin along the plastic strain line and by drawing the parallel line to initial stress strain line under elastic range plus by projecting the obtained point on the stress strain under plastic range to the vertical axis (i.e. along the stress line) as shown in figure 5.11.

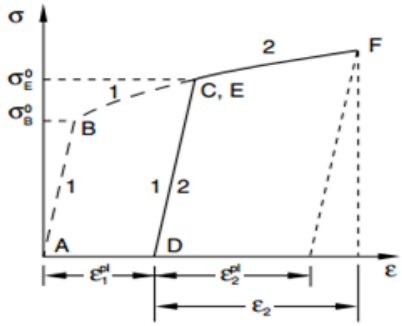

Figure 5.11 Correct Initial yield stress

5.2.4. Stress distribution in cases of elasto plastic modeling

Figure 5.12 below shows the Y-component stress distribution in the elasto plastic modeling. It highlights a stress concentration zone near the sleeper bottom corner. The maximum stress in this zone is over 6.64Mpa. It can also be seen that the vertical stress is concentrated under the sleeper and spreads downwards at a narrow angle.

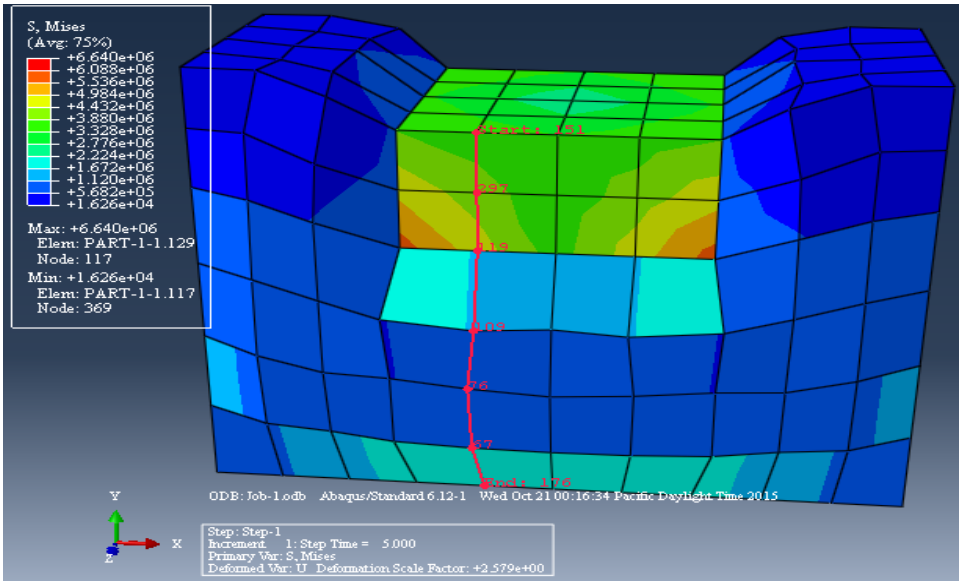

Figure 5.12 (a). Simulation of Stress distributions with created paths

And the figure 5.12(b) below indicates that the stress distribution from the wheel load in various depths of ballast layers. And it shows that stresses are the highest immediately under the sleeper and decline non- linearly with increasing depths.

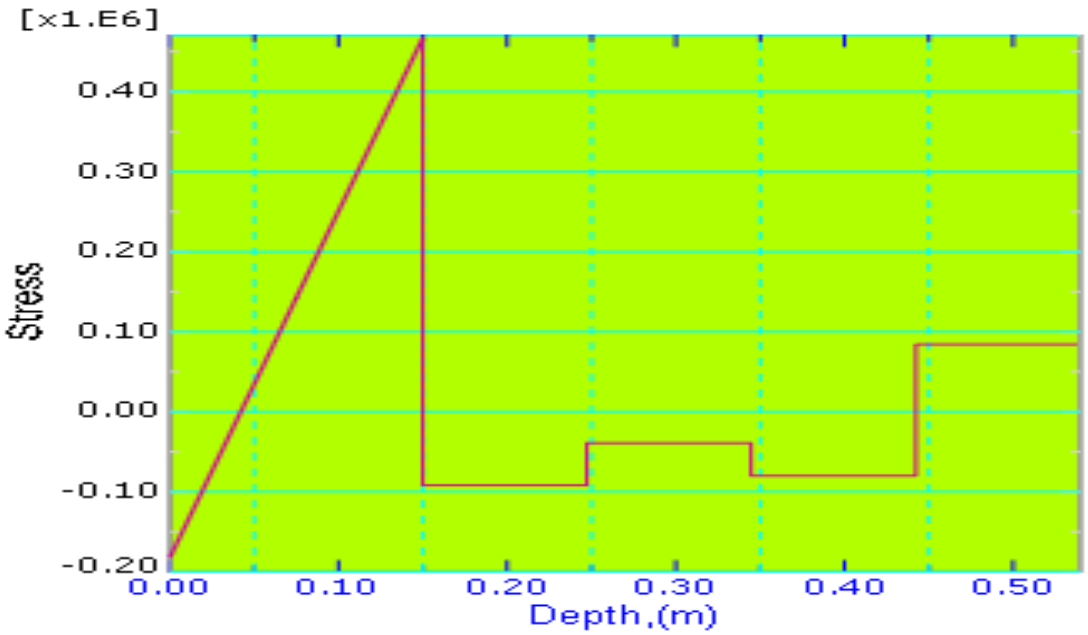

Figure 5.12 (b) Vertical stress distributions in case of elasto plastic deformation along defined paths

5.3. Comparison of Numerical ballast Settlement with empirical Modeling

As it can be observed under numerical modeling, the behavior of ballast specimens under repeated loading was non linear and stress-state dependent. During the first cycle of loading on the sample the axial strain developed rapidly and it recovered only partially up on unloading. Each additional cycle caused an increment of plastic strain, but at a diminishing rate.

Typical variation of settlement of ballast specimen with the number of loading cycles for our case is as shown in figure 5.12. And it can be obtained by using the empirical formula (5.1) ,which is reviewed under literature, to know the settlement of ballast materials after N number of loading cycles , provided that the permanent strain caused by the first load cycle (ε_1) were obtained numerically from the analysis results shown in figure 5.1 and 5.6 above. Where the magnitude of permanent strain caused by the first load cycle (ε_1) in cases of Elastic and elasto plastic cases are 0.67 and 2.781 respectively.

$$\varepsilon_N = \varepsilon_1 (1+C\log N) \quad \ldots\ldots\ldots\ldots\ldots\ldots\ldots\ldots\ldots\ldots (5.1)$$

Based on the settlement equation (5.1) and the permanent strain caused by the first load cycle obtained from the model the permanent deformation of ballast materials we have considered have been analyzed at different number of load repetitions as shown in table 5.3 below.

Table 5.3. : Analysis of Permanent Deformation of Ballast material at repetition of loading

N	logN	C	Clog N	(1+CLOgN)	Elastic Settlement	Plastic settlement
1	0	0.3	0	1	0.67	2.781
10	1	0.3	0.3	1.3	0.871	3.6153
100	2	0.3	0.6	1.6	1.072	4.4496
1000	3	0.3	0.9	1.9	1.273	5.2839
10000	4	0.3	1.2	2.2	1.474	6.1182
100000	5	0.3	1.5	2.5	1.675	6.9525
1000000	6	0.3	1.8	2.8	1.876	7.7868
10000000	7	0.3	2.1	3.1	2.077	8.6211
100000000	8	0.3	2.4	3.4	2.278	9.4554
1000000000	9	0.3	2.7	3.7	2.479	10.2897

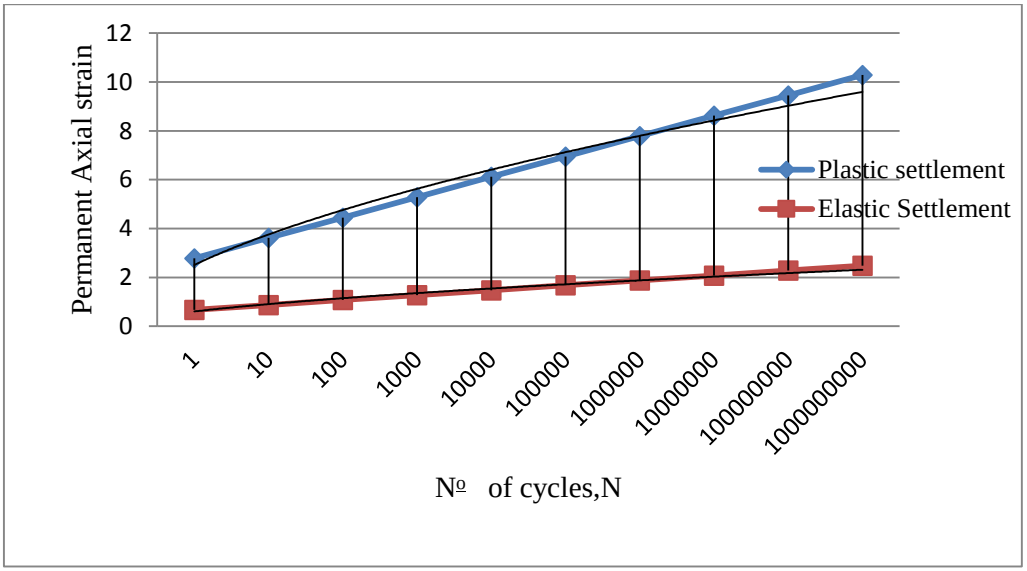

Figure 5.13. Variation of settlement with number of loading cycles under both elastic and plastic cases

The graph obtained from the experimental analysis shows that the cumulative permanent deformation (plastic strain) of ballast material increasing linearly with increasing the repetitions of load, provided that the other parameters affecting the deformation are held constant.

5.3.1. ANALYSING AND DEVELOPING THE SETTLEMENT EQUATION USING EMPIRICAL AND NUMERICAL RESULTS

One of the important part of this topic concerns developing the permanent settlement equations as a function of the number of repetition of loads. It have been tried to develop the permanent deformation of ballast by the using finite element method (FEM) analysis results and the settlement equations, provided that the FEM analysis computes the stress distribution within the ballast and yields initial settlement after first loading. And the settlement equation allows us to calculate the permanent deformation of the ballast under different stress conditions after a certain number of load cycles.

The settlement equations have been developed based on the ballast cyclic simulation. And the settlement results show a high dependence on number of cycles. The ideal settlement equation should be able to predict the permanent deformation as a function of number of load cycles. One of the most common approaches used to predict track settlement is the use of track logarithmic laws which shows the rate of deformations of ballast under repetition of loads.

From analysis, it was found that when the ballast permanent deformation is plotted in a coordinate system of permanent axial strain accumulation rate ($d\varepsilon_a/ dN$) against number of load cycles (N) on logarithmic scales, the plotted curves are approximately straight lines, as shown in Figures 5.14.

Table 5.4. Analysis of rate of permanent Deformation of Ballast material at various repetition of loading

Col. 1	2	3	4	5	6	7	8	9	10	11
N	logN	C	Clog N	(1+CLOg N)	ε_{Ne}	ε_{Np}	Col.6/Col.2	Col.7/(Col. 2)	log(Col 8)	log (Col.9)
1	0	0.3	0	1	0.67	2.78	**1.415***	**5.865***	0.151	0.768
10^1	1	0.3	0.3	1.3	0.871	3.62	0.871	3.615	-0.059	0.558
10^2	2	0.3	0.6	1.6	1.072	4.45	0.536	2.225	-0.271	0.347
10^3	3	0.3	0.9	1.9	1.273	5.28	0.424	1.761	-0.373	0.246
10^4	4	0.3	1.2	2.2	1.474	6.12	0.368	1.529	-0.435	0.185
10^5	5	0.3	1.5	2.5	1.675	6.95	0.335	1.391	-0.475	0.143
10^6	6	0.3	1.8	2.8	1.876	7.78	0.313	1.297	-0.505	0.113
10^7	7	0.3	2.1	3.1	2.077	8.62	0.296	1.231	-0.528	0.090

*…extrapolated results

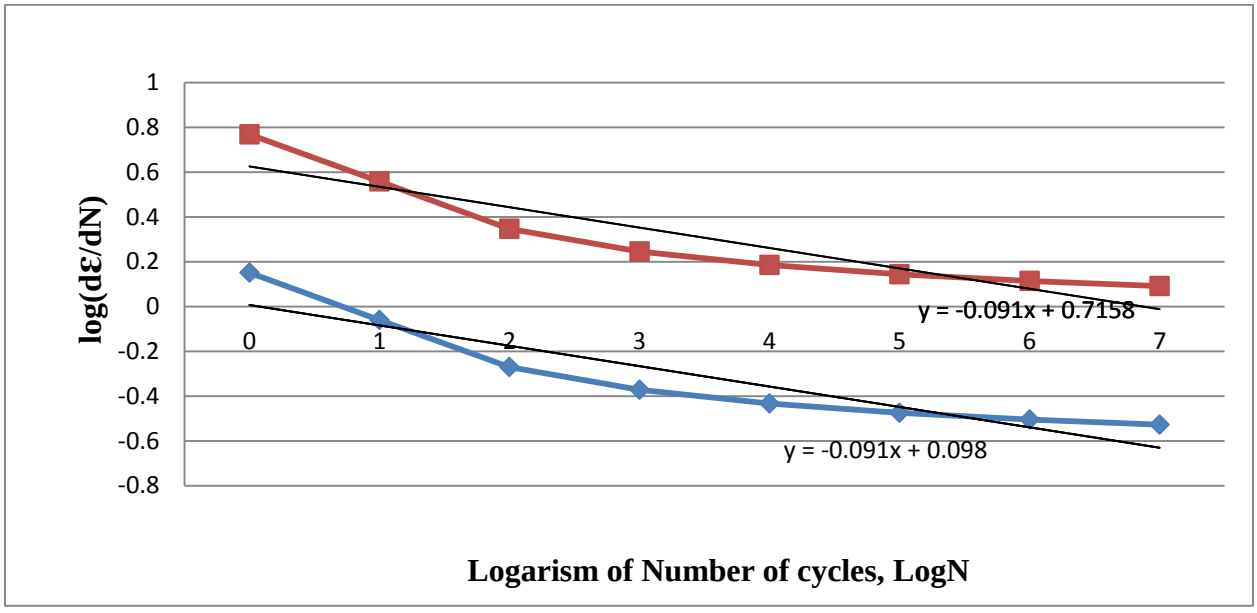

Figure 5.14. Axial strain accumulation rates against number of cycles

Figure 5.14, Shows the axial strain accumulation rate against number of load cycles and it indicates that rate of strain accumulation decreases with increasing number of cycles of loading. Therefore, a linear relationship between log ($d\varepsilon_a/dN$) and log N can be written in the form equation 4.2 below:

$$\text{Log}\left(d\varepsilon_a/dN\right) = A - B\log N \quad \text{---------- (Equation 5.2)}$$

Where A and B are the coefficients. A control the intercepts of these lines, B is the gradient.

By integrating Equation 5.2, the following equation of permanent axial strain (ε_a) can be obtained:

$$\varepsilon a = \frac{10^A}{1-B} N^{1-B} + C \quad \text{---------- (Equation 5.3)}$$

Where C is a constant from integration.

In Equation 5.3, when the number of load cycles (N) equals zero, the permanent axial strain (εa) should be zero as well. Therefore, the constant C can be deleted, and Equation 5.3 becomes:

$$\varepsilon a = \frac{10^A}{1-B} N^{1-B} \quad \text{---------- Equation (5.4)}$$

Coefficients A and B are calibrated using the analysis of permanent deformation of ballast materials mentioned in table 4.4 above. Here the shaded part of figure 5.15 below indicates the exponential permanent deformation of ballast material we have considered.

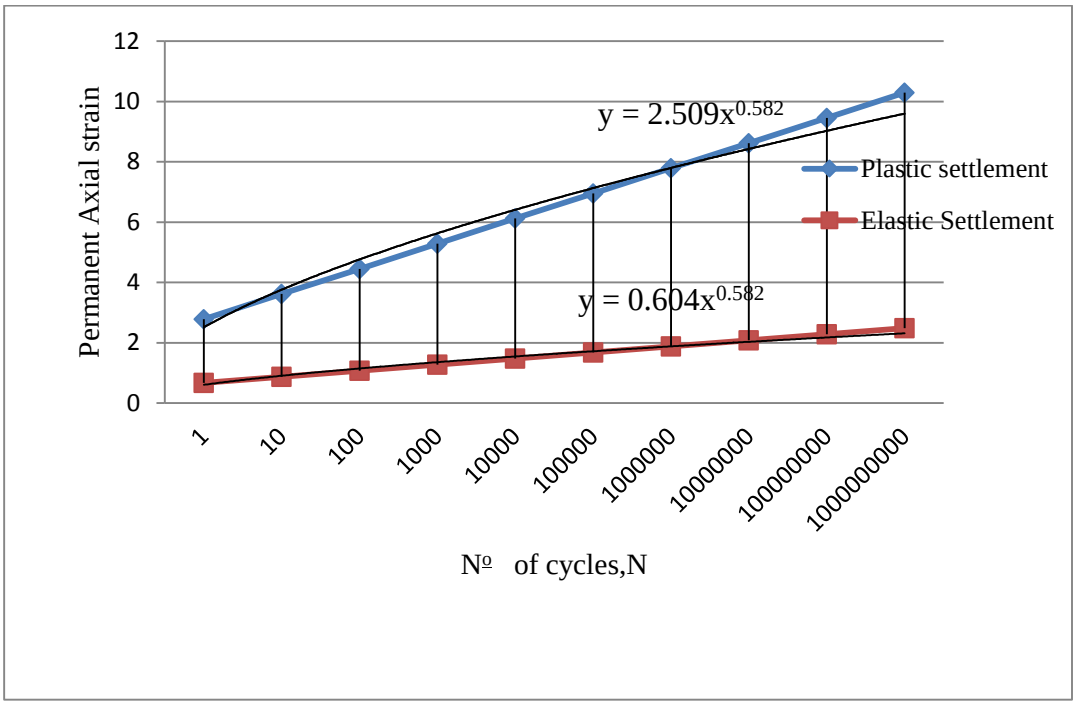

Figure 5.15 Predicted permanent axial strain for the cyclic loading at different number of load cycle, N

The calibrated result shows that permanent axial strain of ballast under cyclic loading is predicted by using:

$$\varepsilon_a = 1.905N^{0.582} \quad \text{.....(Equation 5.5)}$$

Therefore, by equating equation 5.4 and 5.5 simultaneously the coefficients A and B can be obtained. And they are 0.045 and 0.418 respectively.

According to the permanent deformation results of the simulated ballast particles in the FEM, most of the settlement occurred immediately underneath the sleeper. Little settlement was detected from the simulated ballast particles as a depth of ballast is increasing from the edge of the sleeper, as shown in Figure 5.1b. According to the equation 5.4 and the obtained result shown in figure 5.14, the ballast material we have considered have been deform exponentially with

increasing the repetition of loads. But the analysis obtained using empirical formula adopted from the literature indicates that the permanent deformation of ballast materials after number of load repetitions increases linearly with increasing the load repetitions. And using empirical formula requires sophisticated material properties that affect the behavior of ballast materials under cyclic loading. So that predicting the deformation of ballast layers using empirical formula is somewhat a tedious task and it yields in accurate result since it is sensitive to different factors.

As such, if the factors affecting the permanent deformation of ballast are not obtained easily and accurately it is better to use the numerical modeling to predict the permanent deformation of ballast materials under cyclic loading.

Besides, the FEM simulated vertical stress in the model showed that the stress was concentrated under the sleeper and spread downwards at a steep angle. This accumulated stress causes the compaction of ballast materials, particle edge breakage and re arrangement of particles under investigations during cycle of loading. And it is difficult to consider those effects while using experimental formula to predict the permanent deformations.

CHAPTER SIX CONCLUSION AND RECOMMENDATION

6.1. CONCLUSION

It can be observed that Finite element method (FEM) is one of the most versatile numerical techniques for engineering analysis, as it enables a good approximation to be made even when a system exhibits non-linear material behavior.

The permanent deformation, or settlement, of railway ballast is complicated under cyclic wheel load, as large plastic deformation and degradation usually happen in the process. The numerical analysis method used herein is not capable of simulating the plastic deformation accumulation and degradation under cyclic load. However, the FEM analysis provides the information to predict railway ballast deformation in terms of number of loading under wheel loading. The prediction of ballast stress conditions has been completed utilizing material models readily available in the commercial finite element program ABAQUS. In the initial modeling, the box test was simulated to investigate the ballast response under monotonic loading with an elastic material model. However, it was found that the use of a linear elastic material model was not sufficient to simulate ballast behavior. Then, a more detailed analysis using the extended Drucker-Prager model with hardening was carried out. Eventually, FEM simulations of the elasto plastic were carried out to investigate stress distributions. And we found that both vertical and horizontal stresses were concentrated underneath the sleeper in both modeling.

Besides, it can be observed that more of the vertical deformation of track resulted from the settlement of ballast materials under the sleeper. And it can be concluded that, the maximum deformation of ballast layer is observed during elasto plastic modeling technique since the

yielding of materials is considered under elasto plastic cases. Also we have seen that the analysis of ballast response using elasto plastic yielding requires the elastic property of ballast materials to account the elastic response of ballast materials up to the yielding points during the analysis.

To capture the yield stress hardening features of ballast materials under consideration during cyclic loading it is essential to use the extended Drucker-Prager model with hardening in FEM simulations. The simulation provides the stress levels within the ballast, which were used in settlement equations to compute ballast settlement after, N, number of load repetitions.

Generally from our model, it is possible to conclude from the experimental result that, though the axial strain accumulation rate of sample of ballast material under cyclic loading is decreasing with increasing the load repetition the permanent deformation (overall settlement) of ballast material under the cyclic loading can be increased exponentially with increasing the number of load repetition. But the numerical result we have obtained from the analysis shows that, the permanent deformation of ballast materials under considerations deform non- linearly with number of load repetitions.

6.2. RECOMMENDATIONS FOR FURTHER STUDY

This thesis has presented a method to predict the permanent deformation of railway ballast, after, N, number of load repetitions. And the following issues are recommended for future research.

A. Availability of data

It is recommended that all input data to the soft ware , especially ballast materials property modeling, requires sophisticated and accurate data to run and obtain the accurate model, so that, before modeling is taking place trail axial test should be conducted in order to get the actual

data that represent the site under investigations for case study analysis. Further tests should be carried out at each stress condition to check repeatability, and accuracy of the data.

B. FEM Analysis and Modeling

An increased ability to simulate actual railway track is necessary, and additional influences should be introduced into the model. Moving multi-wheel loads on the rails could be applied on top of the sleepers to mimic moving train wheels. Therefore, further research is required to develop more computational techniques that can simulate the buildup of stress under multi-cyclic load.

C. Material simulation

Ballast material is a collection of distinct particles which displace relative to each other, and forces between particles only exist when there is a contact between particles exists. But our models consider the ballast material as a solid body which was approximated to reality. Therefore, further research is required to develop more appropriate material models particularly; Discrete Element Modeling simulation is an alternative method that should be recommended.

D. Test machines

The deformation of ballast material under cyclic loading may also be determined by using laboratory tests under various deviator stresses and confining pressures. So that the availability of trailxail machine in university is mandatory to calibrate and compare test result with the software simulation.

REFERENCES

1. Abaqus 6.12.1, Analysis User's Manual Volume III: Materials, Software Manual
2. Alva-Hurtado, J.E. and Selig, E.T., (1981). "Permanent Strain Behaviour of Railroad Ballast". Proc. of 10th International Conference on Soil Mechanics and Foundation Engineering, Stockholm, Sweden, Vol. 1, 543-546, 1981. A. A. Balkema, Rotterdam, the Netherlands.
3. Boyce, J.R., Brown, S.F., and Pell, P.S., (1976). "The Resilient Behavior of a Granular Material under Repeated Loading." Proceedings Australian Road Research Board, 8, pp. 8-19.
4. Chiara Paderno, LAVOC – EPFL, (9th Swiss Transport research conference paper STRC 2009).
5. Chaitanya Calla,(December 2003). "Two layered ballast system for improved performance of railway track" University of Coventry for the Degree of Doctor of Philosophy.
6. Chen, W.F. (1994). Constitutive Equations for Engineering Materials, Elsevier,New York.
7. A. Higgins, "Scheduling of Railway Track Maintenance Activities and Crews," Journal of Operational Research Society, vol. 49, no. 10, pp. 1026–1033, 1998.
8. F. Beichelt and K. Fischer, "General Failure Model Applied to Preventive Maintenance Policies," IEEE Transactions on Reliability, vol. R-29, no. 1, pp. 39–41, 1980.
9. HL Theyse,"Mechanistic-Emperical modeling of the permanent deformation of unbound pavement layers," Division of Roads and transport Technology, Pretoria, South Africa.
10. Ishikawa, T. Sekine, E. (2002) Effect of Moving Wheel Load on Cyclic Deformation of Railroad Ballast, Proceedings of International Railway Engineering Conference, Edinburgh, ECS Publications

11. J. Sadeghi and H. Askarinejad, “Development of improved railway track degradation models,” Structure and Infrastructure Engineering, no. 6, pp. 675-688, 2010.
12. Knutson, R.N., (1976). Factors Influencing the Repeated Load Behaviors of Railway Ballast. PhD Dissertation, University of Illinois at Urbana-Champaign.
13. Leeves C.G., (1992) Standards for Track Components, Cost Effective Maintenance of Railway Track, London, Thomas Telford.
14. Lekarp, F., (1997). Permanent Deformation Behaviour of Unbound Granular Materials. Licentiate Thesis, Royal Institute of Technology, Stockholm.
15. Lekarp, F. and Dawson, A., (1998). "Modelling Permanent Deformation Behavior of Unbound Granular Materials." Construction and Building Materials 12, No. 1, 9-18.
16. Lim, Wee Loon. 2004. “Mechanics of Railway Ballast Behaviour”. The University of Nottingham.
17. M. Andersson, “Strategic Planning of Track Maintenance - State of the Art,” Department of Infrastructure, Royal Institute of Technology, TRITA-INFRA 02-035, 2002
18. MD WADUDSALIM, (2004), “Deformation and Degradation Aspect of ballast and constitutive modeling under cyclic loading”,UNIVERSITY OF WOLLONGONG,
19. Office for Research and Experiments (ORE), (1970). "Stresses in Rails, the Ballast and the Formation Resulting from Traffic Loads." Question D71, Report No. 10, Vols. 1 and 2, International Union of railways, Utrecht, Netherlands.
20. Shenton, M J. 1975. “Deformation of Railway Ballast Under Repeated Loading Conditions.” In Railroad Track Mechanics and Technology, 1–26. Princeton University.

21. S. Simson, L. Ferreira, and M. Murray, “Rail Track Maintenance Planning: An Assessment Model,” Transportation Research Record: Journal of the Transportation Research Board, no. 1713, pp. 29–35, 2000.
22. Talbot, A N. 1980. Stresses in Railroad Track - The Talbot Reports. American Railway Engineering Associations.
23. Xiaoyi Shi , (April 2009) ,Prediction of permanent deformation in railway track, University of Nottingham,
24. W.-J. Zwanenburg, “Modelling Degradation Processes of Switches and Crossing for Maintenance and Renewal Planning on the Swiss Railway Network”, in Civil Engineering, Ecole Polytechnique Federale de Lausanne, 2009.
25. Y. Sato,“Japanese Studies on deterioration of ballasted track,” Vehicle System Dynamics, vol.24 (sup1), pp. 197-208, 1995.
26. Zaman, M., Chen, D.H., and Laguros, J., (1994). "Resilient Moduli of Granular Materials." Journal of Transportation Engineering, 120 (6), pp. 967-988.